International Journal of Science and Engineering Applications
Volume 10-Issue 11, 148 - 151, 2021, ISSN:- 2319 - 7560

Antifungal Efficacy of Allium Sativum and Zingiber Officinale on Fungi Isolated from Spoilt Bread

Jamilu, H.
Department Of Applied Biology, Kaduna Polytechnic Nigeria

Hussain, F.I.
Yusuf Maitama University Kano, Nigeria

Ibrahim, T.
Ahmadu Bello University Zaria, Nigeria

Abstract: *Zingiber officinale* is a common condiment for various foods and beverages and a history of important traditional medicine herb for the treatment of stomach disorder. This study deals with the antifungal activity of *Allium sativum* and *Zingiber officinale* and their phytochemical composition. Ethanolic extracts of two spices *(Allium sativum and Zingiber officinale)* were tested for antifungal activities against *Aspergillus* sp, *Penicillium* sp and *Fusarium* sp using mycelia growth extension method, result showed varying degrees of antifungal activities against the test fungi. The two extracts showed similar pattern of antifungal activities on the test fungi withthe extract of *Allium sativum* being more effective with increased zones of inhibition with increased concentrations. Phytochemical screening revealed the presence of flavonoids, saponins, terpenoids and tannin for *Allium sativum* and flavonoids, glycosides, tannins and anthraquinone for *Zingiber officinale*. The significant growth of inhibitions of the test fungi by the plant extract suggest the possible use of these spices in controlling infections caused by these fungi and food spoilage.

Keywords**:** *Allium sativum, Zingiber officinale,* Ethanolic extract, Phytochemical screening.

1. INTRODUCTION

Historically, medicinal plants have been a source of novel drug compounds, plants derived products have made large contributions to human health and wellbeing.

Over the years, much efforts have been devoted tothe search for new antimicrobial agents from natural sources such as plants and others for treatment and for food preservations. Many scientists across the globe have reported antimicrobial properties of several medicinal plants but still a very meager portion of this tremendous potential drug-repertoire has been scientifically screened ().

Spices and herbs have been used as food additives since ancient time, as flavouring agents and also as natural food preservatives (Mariya *et al*., 2009). They serve as item of international commerce for many hundred years. Several spice extracts have broad spectrum antimicrobial properties and can be recognized as bio-preservatives, having no harmful effect on human health (Akponah *et al.*, 2013). Many of these spice extracts possess significant antimicrobial activity which in many cases is due primarily to particular constituent such as alkaloid phenols, glycosides, steroids, tannins or essential oils (Lopez et al., 2006). A number of spices show antimicrobial activity against different types of microorganisms and these activities depend on the microorganism, the type of specie, the test method as well as the chemical composition and content of extracts and essential oils (Laura, 2007). Among these specie which are available and cheaper than the conventional drugs include garlic and ginger which in their natural states are widely used in West Africa as herbal medicine in the nineteenth century, ginger served as a popular remedy for cough and asthma when the juice is mixed with little juice of fresh garlic and honey (Foster, 2000).

Zingiber officinale belongs to the family *Zingiberaceae* while *Allium sativum* on the other hand belongs to the family *Alluaceae*, they have been used for decades in treating cold induced diseases such as nausea, asthma, cough, hearth palpitation, swelling, dyspepsia, loss of appetite and rheumatism (Foster, 2000).

The anti-inflammatory properties of ginger and garlic have been known and valued for centuries. The original discovery of ginger's inhibitory effects on prostaglandin biosynthesis in the early 1970s has been repeatedly confirmed. This discovery identified ginger as a herbal medicine product that shares pharmacological properties with non-steroidal anti-inflammatory drugs. Ginger is a strong anti-oxidant substance and may either mitigate or prevent generation of free radicals. It is considered a safe herbal medicine with only few and insignificant adverse/side effect.

The approved modern the rapeutic applications for ginger are supportable based on its history of use in an established systems of traditional and conventional medicine, extensive phytochemical investigation, pharmacological studies in animals and human clinical studies.

This study was aimed at evaluating the Antifungal potential of *Zingiber officinale* and *Alliumsativum* against *Penicillium* species, *Fusarium* species and *Aspergillus* species.

2. MATERIALS AND METHODS

This research was carried out in the Department of Applied Science, Microbiology Laboratory of Kaduna Polytechnic.

Collection and Handling of Plant Materials

The *Allium sativum* and *Zingiber officinale* were purchased in Central Market in Kaduna State, Nigeria. The authentication of the species was done by comparing them with the voucher specimens available in Department of Biological Science Faculty of Life Science, Ahmadu Bello University, Zaria, in an air tight container. The samples were conveyed to the Microbiology Laboratory Department of Applied Science, Kaduna Polytechnic until required.

Plant Extraction

The *Allium sativum* bulbs and *Zingiber officinale* rhizomes were separately washed with distilled water and aseptically peeled with a sterile knife. They were crushed separately using sterile mortar and pestle, and transferred into two stoppered vessels. Five hundred (500ml) of ethanol was poured into each of the vessels containing the crushed sample and the system were allowed to stand for a day without shaking after which the system was subjected to occasional shaking for another six days. The liquids were then strained off and filtered using Whatman no 1 filter paper. The recovered filtrates were evaporated using water bath and resultant crude extracts were used for antifungal activity testing.

Isolation of Test Organisms

The Aspergillus, Penicillium and the Fusarium species were isolated from spoilt bread using Sabouraud's Dextrose Agar. Different colours were observed on the spoilt bread as a result of different fungal growth,they were inoculated on petri dishes containing solidified Sabouraud Dextrose Agar. They were incubated at room temperature for 5 days, the resultant mixed cultures were subcultured so as to obtain pure cultures.

Macroscopic Identification of the Fungal Isolates

The fungal isolates were identified macroscopically using cultural appearance and cultural characteristics with the aid of a hand lens. Different colours such as black, green, pink and white were seen on the plates.

Microscopic Identification Using Lactophenol

The Smears from the culture were prepared and stained with lactophenol. The preparations were observed under x10 and x40 objectives of the microscope and compared with the fungi identification key for inference.

Phytochemical Screening of the Extracts

Phytochemical screening was carried out on the two extracts using the standard methods.

Test for Saponin

Exactly 5g each of the two extracts were accurately measure and transferred into 5ml distilled water to two separate test tubes. A frothing appearance on shaking with water indicates the presence of saponin.

Test for Tannins

Five (5ml) each of the two extracts were accurately measured and transferred into 10ml distilled water in two separate test tubes; ferric chloride reagent was added. Blue black or blue green precipitate appearance indicates the presence of tannin.

Test for Flavonoids.

In order to test flavonoids, 5ml each diluted ammonia solution was added into 5ml each of the extract in separate test tubes. 3ml of concentrate $H_2S0_4$was added, a yellow coloration indicates the presence of flavonoids.

Test for Terpenoids

Two grams (2ml) each of chloroform was added into 1ml of the extracts in separate test tubes and 3ml of concentrated $H_2S0_4$was added, a reddish-brown coloration at the interface indicate the presence of terpenoids.

Test of Steroids

Two (2ml) each of acetic anhydride was added to 3ml each of the two extracts in a separate test tubes and 2ml of sulphuric acid was added by the sides of the test tubes. A color change of violet or blue indicated the presence of steroids.

Test for Anthraquinone

Exactly 5g/ml each of the two extracts were taken into a dry test tube and 5ml of chloroform was added shaken for 5 minutes. Equal volume of 10% ammonia solution was added into the test tube. A pink violet or red colour in the ammonical layer (lower layer) indicates the presence of anthraquinone.

Test for Glycosides

Five (5ml) each of the two extracts were dissolved in 1ml of glacial acetic containing one drop of ferric chloride solution. 1ml of concentrated sulphuric acid was added into the test tube. A brown ring obtained at the interface indicates the presence of glycosides.

Determination of Plant Yield

The percentage yield was obtained using the formula $^{w1}/_{w2}$ x $\frac{100}{1}$. Where$w1$ is the initial is weight of the sample before extraction and $w2$is the final weight of the sample afterextraction.

Antifungal Testing

The effect of the spice extracts was determined by measuring the mycelial extension of the fungi on Sabouraud's Agar medium, 2ml each of the spice extract was mixed with 200ml of sterile Sabouraud's Dextrose Agar medium in test tubes and poured into sterile petri dishes. Streptomycin, 0.5mg/litre was prepared and was added to the mixture of the medium and the spices to suppress the growth bacteria. The plants were allowed to cool and solidified while the test organisms were inoculated into the medium. Mycelial disc (5mm in diameter) was collected on the surface of actively growing fungal culture using a sterile cork borer and was placed at the central of the medium containing the extract. Two plates were prepared for each spice and for each fungus under aseptic conditions. The control plates without the spice extracts were similar inoculated with the fungi. The set up were incubated at room temperature for five days in the laboratory. The radial growth less the diameter of the initial inocula was measured in two directions along the perpendicular lines and the means were calculated for each plate and with the fungal growth.

Preparation of Varied Concentrations of the Extract

Different concentrations of the two extracts were prepared using distilled water. Exactly 0.1g each of the extracts were dissolved in 10ml each of the distilled water in a test tube to obtain the 100mg concentration. Exactly 5ml was taken from the 100mg concentration and dispensed into 5ml of distilled water to get the 50ml/ml concentration. Another 5ml was also taken from the 40mg concentration and dispensed into 5ml of distilled water to obtain the 25mg concentration and finally 5ml was taken from the 25mg concentration and dispensed into 5ml of distilled water to obtain the 12.5 concentration. Four different concentrations (100mg, 59mg, 25mg and 11.5g) were prepare for each of the extracts and these varied concentration were used against the isolates to determine the Minimum Inhibitory Concentration (MIC) (Cheesbrough, 1994).

Determination of Minimum Inhibitory Concentration of Spice Extract

Exactly 20ml of Sabouraud's Dextroxe Agar was poured into sterile petri dishes containing different concentration (100mg, 50mg and 12mg) of the respective extracts of the species (Ginger and garlic) Mycelial discs (5mm in diameter) was collected from the surface of actively growing fungal culture using a sterile cork borer and was placed at the centre of the Sabouraud's Dextrose Agar medium containing the extract. The Minimum inhibitory Concentration (MIC) was determined as the least concentration of spice extract that showed an inhibitory effect in the mycelial growth of the test fungi when compared with the control using the radial growth method (Cheesbrough, 1994).

Determination of the Minimum Fungicidal Concentration of the Extracts

The *in vitro*fungicidal activities were determined for each plant extract. After 72 hours of incubation, 1ml was subcultured from each culture that showed complete inhibition (100% or an optically clear plate), from the last positive culture (growth similar to the growth on the control culture and from the growth control (Extract free medium) on to Sabouraud's Dextrose Agar plates and were incubated at room temperature until growth was seen before 48hours. The Minimum Fungicidal Concentration (MFC) was determined as the lowest concentration that showed no growth of fewer than 3 colonies.

3 RESULTS AND DISCUSSIONS

RESULT AND DISCUSSION

Table 1: Percentage Yield of the Spice Extracts in Ethanol

Extract	**Weight 1 (w1)**	**Weight 2 (w2)**	**Yield &**
Allium Sativum	20kg	15kg	13.33%
Zingerber officinale	20kg	13kg	15.38%

Table 2: Phytochemical properties of *Allium sativum* and *Zingiber officinale* Extracts.

Extracts	Phytochemical screening						
	Flavonoid	Terpenoids	Saponins	Glycoside	Glycoside Tannins	Steroids	Anthraquinone
Allium sativum	+	+	+	-	+	-	+
Zingiber offic inal e	+	-	+	+	+	-	_

Table 3: Antifungal activity of Allium sativum and Zingiber officinale extract (diameter of mycelia extension) (mm)

Extract	Test Organism		
	Penicillium	Aspergillus	Fusarium
Allium sativum	25	17	5
Zingiber officinale	25.5	19	8.5

Table 4: Minimum Inhibitory Minimum Fungicidal Concentration of Allium Sativum (mg/ml)

Organisms	Concentration				
	0	12.5	25	50	100
Penicillium Specie	+	+			-
Aspergillus Specie	+	+	+	+	-
Fusarium Specie	+	+	+	-	-

Table 5: Minimum Inhibitory Minimum Fungicidal Concentration of Zingiber officinale Extract (mg/ml)

Organisms	Concentration				
	0	12.5	25	50	100
Penicillium Specie (mm)	+	+	+	-	-
Aspergilles Specie	+	+	+	+	-
Fusarium Specie	+	+	-	-	-

The percentage yield of the extract of *Alliumsativum* was found to be 13.33% while that of *Zingiberofficinale* was 15.38%. However the result in table 1 showed a wide range of yield among the two extract with *Alliumsativum*having a lower percentage yield and Zingiber officinale revealed the presence of some bioactive compounds which are responsible for their antifungal activities. This result is similar to the report of Roy et al., (2006) who observed that the phytochemical constituents of *Allium sativum* are responsible for

its antifungal properties. The antifungal evaluation of ethanolic extracts of *Allium sativum*and Zingiber officinale revealed a significant antifungal potency against the test organisms. Varying degrees of antifungal activities by the two extracts were observed at different concentrations, the spices showed antifungal activity against the fungi tested. *Fusarium*specie was observed as the most susceptible fungus while *Penicillium*specie was the least susceptible

fungus to the crude extracts of both spices as shown in table 3. Results showed that the two spices have similar antifungus activates the test fungi (Table 3). Both spices were also observed to have similar Minimum Inhibitory Concentration against *Fusarium*specie at 50mg/ml compared with *Zingiberofficinale*which have Minimum Inhibitory Concentration at 100mg/ml against *Fusarium* species. The strong inhibition potential of *Zingiberofficinale*is attributed to the fact that it contains over 400 different compounds, a mixture of both volatile and non-volatile chemical constituents such as Zingerons, shigaols, gingerols, sesquiterpenoids and a small monoterpenoid fraction (Chrebasik et al., 2005). The antifungal activity of garlic extract is found to be very effective in inhibiting the growth of *Aspergillums* species (Dankert et al., 2009)

The antimicrobial activity of extracts of Allium sativum have lobe been linked to the presence of some bioactive compounds, these secondary metabolite also serve to protect the plants themselves against bacterial fungal and viral infections (EL-Mahmood and Amey, 2007). These bioactive compounds are known to work synergistically to produce various effects on the human and animal subjects (Amagase, 2006). The antifungal potency of these spices also supported the work of Udo et al., (2001) who reported that methanol and ethanol extracts of*Alliumsativum*have high potency for the control of pathogenic fungi in potato and yam and tubers. In this study, it was observed that the higher of concentration of the ethanolic extracts of the spices, the higher the potency in the inhibition of mycelial growth of the fungi tested (Table 4). The Minimum Fungicidal Concentration against the test isolates was established for the two extracts in table 4.5. The two extracts showed fungicidal activities against the test isolates at 100mg/ml concentration except of *Alliumsativum*which showed a fungicidal activity on *Fusarium* specie at 50mg/ml (Banso et al., 1999). Reported that the antifungal substances contain in the extracts were fungicidal at higher concentrations. This study indicate the Minimum Fungicidal Concentration than in the Minimum inhibitory concentration assays but not at lower concentration as shown in Table 5.

4.0 CONCLUSION

This study has demonstrated the effectiveness of *Alliums ativum*and *Zingiber officinale* extracts against *Aspergillus* species, *Penicillium* species and *Fusarium*species. This has provided justification that if well processed, *Alliums ativum* and *Zingiberofficinale*can be used to develop bioactive substances that may have promising effect on the treatment of some infections. The extracts exhibit fungicidal properties that support their traditional use as antimicrobial (Cowan, 1999). *Allium sativum* and *Zingiber officinale* therefore have great potentials for the development of antimicrobial drugs most especially for the treatment of fungal infections.

RECOMMENDATIONS

Based on the major findings of the study, the following recommendations were made;

1. Further work on the phytoconstituents, isolation, purification and characterization of the bioactive components of these plants is recommended as it could lead to the development of more effective substances that can be used to treat infections.

2. It has been found in this study that *Alliumsativum* and *Zingiberofficinale* extracts possess antifungal potency, it is more therefore imperative that phymaceutical companies should explore them as a source of antifungal drugs.

3. *Alliumsativum* and *Zingiberofficinale* should be included as constituents in drugs formulation.

REFERENCES

1. Akponah, E., Okoro, I.O., Ubogu, M. and Ejukonemu F.E (2013); Anti-inflammatory and Anti-odidant properties of Ginger and Garlic. *International Journal of Agricultural policy and Research* 1:177-204.
2. Amagase H., (2006). Clarifying the real Bioactive Constituent of Garlic. Journal of Nutrition 136:716-725.
3. Banso, A., S.O Adeyemo and P.Jeremaiah properties of Spice Extracts. *Journal of Applied science and Management* 3:9-11.
4. Chesbrough, I. (2004); Antifungal properties of some Locally Used Spices in Nigeria against Some Rot Fungi. *African journal of plant Science* 3:139-141.
5. Chrubasik, S., Pittler, M.H and Roufogalis, B.D (2005); Zingiberis rhizome: A Comprehensive Review on the Ginger Effect and Efficacy Profiles. Phytimedicine: 12 (9): 684-701).
6. Cowam, M.M. (1999); Plant Products as Antimicrobial Agents. *Clinical Microbiology Reviews* 10:564-582.
7. Dankert, J., Tromp F.J., Deveries, H and Klasen, H.J. (2009); Antimicrobial Activity of Crude Juices of *Allium sativum. Journal of Food Control* 15:479-483.
8. Laura, L. and Zaika M., (2007); Spices and Herbs; Their Antimicrobial Activity and its Determination. *Journal of Food Safety* 9:176-181.
9. Lopez-Malo, A.J., BArreto-Cadivieso, E. and Marin F.S (2006). Aspergillus flavus Growth Reponses of Cinnamon Extract and Sodium Benzoate Mixtures. *Journal of Food Control* 18:1358-1362.
10. Mariya, M., Steirinjar, O., and Nebena, T. (2009); Antimicrobial Effects of Spices and Herbs Essential Oils. *African Journal of Plant Science* 2:139-141.
11. Roy, J., Shekaya, D.M., Callery P.S and Thomas J.G (2006); Chemical Constituents and Antimicrobial Activity of a Traditional Herb Medical Containing Garlic and Black Cumen. *African Journal Traditional*. 20:1-7.
12. Udo, S.E., Madunagu, B.E., and Isemin, C.D. (2001); Inhibition of Growth and Sporulation of Fungal Pathogens on Sweet Potato and Yam by Garlic Extracts. *Nigerian Journal of Biotechnology* 14:35-39.

International Journal of Science and Engineering Applications
Volume 10-Issue 11, 152 - 162, 2021, ISSN:- 2319 - 7560

Finite Element Analysis of End Effector for an Automated Equipment of High-Speed Forming of Thin-Layered Composite Materials

Jake Reeves
Department of Mechanical Engineering
Mississippi State University
Mississippi State, MS 39762,
United States

Dam Kim
Department of Mechanical Engineering
Mississippi State University
Mississippi State, MS 39762,
United States

Yucheng Liu
Department of Mechanical Engineering
South Dakota State University
Brookings, SD, 57007, United States

Youssef Hammi
Department of Mechanical Engineering
Mississippi State University
Mississippi State, MS 39762
United States

Abstract: The present study examines the design of an automated equipment system that will be able to form thin-layered composite materials over a highly complex shape in a very short time interval. The end effector is one of the most essential components of the automated equipment. It is connected to an assembly which is connected to a motorized arm which controls its motion in the y- and z-directions. The end effector is a component that holds an air pressurized fire hose, which is being used as the forming device of this automated forming device. As a result, the end effector will have to be able to hold and contain a highly pressurized fire hose while applying forces in a variety of directions depending on the shape of the forming mandrel. A computational approach using finite element analysis (FEA) was used to examine the end effector materials and the assembly to confirm that they are robust enough to withstand the internal and external stresses and forces without failure or permanent deformation of the end effector materials, forces which are created from the pressurized fire hose and reactive force on the fire hose from the pressure being applied to an independent tool. This means that the automated equipment is capable of forming complex composite laminates in a rapid time without resulting defects.

Keywords: Finite element analysis (FEA), automated equipment, end effector, ethylene propylene diene monomer (EPDM) rubber, composite material

1. INTRODUCTION

The purpose of this study is to determine the stresses and deformation that the end effector of an automated equipment system for high-speed forming thin-layered composite materials will incur during the operation of the system. This automated equipment system will be employed to form the thin-layered composite materials with a highly complex shape in fast cycle times. The system is made up of several components and this study will focus on the end effector, a key component which consists of actuated arm end plates, a rod end attach block, a base plate, a pivot rod end assembly, shaft blocks, a hose plate assembly, and a fire hose (Fig. 1).

In composites manufacturing there are several different types of material equipment; two being material laying equipment and material forming equipment. Material laying equipment are CNC machines with programmable axis movements, rack and pinion and/or linear motor axis drives, and "delivery heads" to dispense the prepreg composite materials. Prepreg material is a carbon fiber material pre-impregnated with resin. The machines are programmed to follow the exact contour of the part tool and lay the prepreg materials onto the tool surface. Automated Tape Layers (ATL) and Automated Fiber Placement (AFP) are commonly material laying equipment used for many aerospace applications like wing skins, spars, ribs, stringers, and fixed trailing edges. ATL and AFP systems are primarily the "material delivery head" technology as there is nothing magic about machine tools. CNC machine tool technology has been used for many years [1].

This research closely aligns with material forming equipment which takes the material that has been laid into flat shapes and pushes it into complex shapes and geometries. Forming equipment often work hand in hand with materials laying equipment, being one of the very next steps in the process. The process of forming composite material in this research process is an automated machine forming machine that takes a flat single ply or thin laminate of prepreg material and presses it into contour and shape. Then repeating the process over and over again on top of itself until the full thickness of the desired laminate is reached. The basis of the end effector is from the historical forming processes developed by The Boeing Company [2-3]. The reason that these methods have been targeted for this research is due its proven effectiveness to form composite materials. Composite materials are extremely difficulty while maintaining laminate quality.

Forming prepreg composite laminates are most subjected to fiber wrinkles during the forming process if they are not properly supported and constrained. Fiber wrinkles in carbon fiber reinforced polymer (CFRP) materials have shown reduction in tensile strengths by 36-40% [4]. With such drastic decreases in strength, it is extremely important to pay close attention to the part quality when manufacturing CFRP parts.

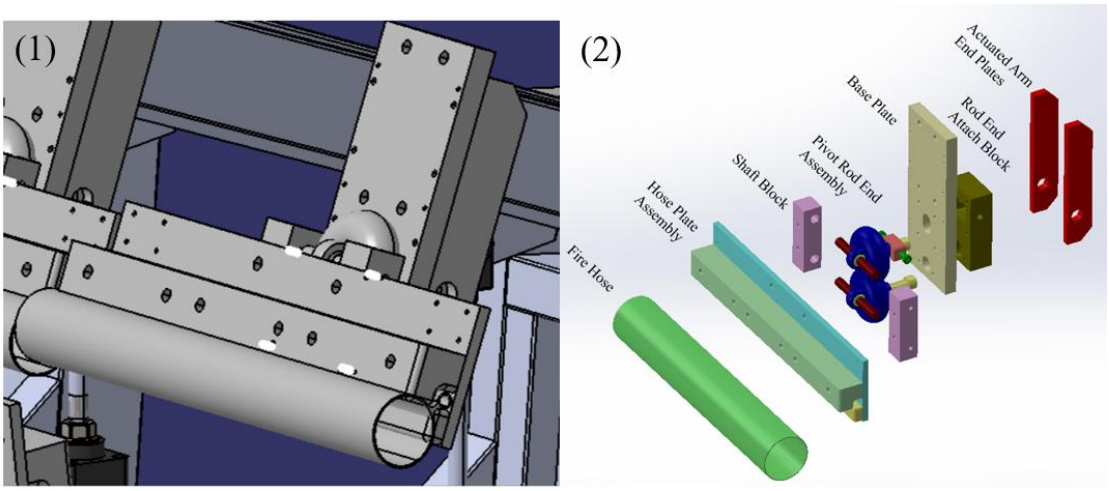

Figure 1. (L) an end effector assembly; (R) its component list

The radius of curvature that the fire hose of the end effector will have to go over will range from 1000 in and 6000 in (25.4 m to 152.4 m). This is the current engineering design that covers most of the curvatures for commercial airplane wing stringers. For this study we will focus on one segment of the end effector which is 23.5 in (59.69 cm) long. The reason of focusing on one section is that the results should be the same but the computing time can be reduced by only looking at one section instead of the entire assembly.

The design of the end effector system is critical in order to ensure that the fire hose, hose plate and assembly components will be able to withstand the different stresses and deformation that will be subject to while fabricating high quality composite laminates. The stresses will be the internal pressure applied to the fire hose and any deflection that the hose plate assembly might incur from the internal fire hose pressure combined with the z-directional applied forced reacted against the fire hose from forming against the forming contour tool.

This equipment will only be handling uncured composite materials; uncured composites are the composite materials that have not yet gone through an autoclave process with heat and pressure to put the laminate in its final cured state. The laminate will have come from an ATL machine, laminating a single ply or thin laminate on a carrier film to be discarded or recycled after each forming cycle. In a production environment, the forming cycles are repeated until maximum thickness is reached and then the formed laminates are assembled together and placed on a cure tool with caul plates and cured into shape. There are several key factors in shaping uncured composite materials; including composite material type (matrix and resin material properties), thickness of composite plies, tooling/support of the composite materials, overall forming pressure and speed as well as consistent/uniform pressure and speed. If the laminates are formed while not adjusting the parameters to these key factors, wrinkles will be induced into the fabricated composite materials which drastically affect the strength and performance of the final composite parts. Some wrinkles are allowed under special circumstances, but typical research and testing is performed with the goal to completely eliminate and prevent any wrinkles from forming. In this research the goal is to form laminates into contour with no wrinkles present.

Figure 2. Wrinkles appear on uncured composite laminates

Other common defects in inadequately formed composites include non-uniform laminate thickness (too thick or too thin), porosity, delamination, and marcelling, etc. To prevent those defects from occurring the equipment needs to be properly calibrated to apply an appropriate amount of pressure on the composite material so that the fire hose can hold the composite laminate in place while forming it over the contour of the forming tool and over a ¼" (6.35 mm) radius which is built into the tool. This radius is part of the wing stringer configuration. The fire hose will be inflated to about 10-15 PSI (~69-103 kPa) and will apply a downward force of 1000-2000 pounds (~4500-9000 N) onto laminate which is on a contoured forming tool. The steps for this automated forming process are illustrated in Fig. 3.

Step 1: Place a laminate on the contoured forming blocks.

Step 2: The pressurized fire hose is lowered onto the laminate and clamps the laminate into a place on the contoured forming blocks with a downward force of 4500-9000 N.

Step 3: The pressurized forming blocks sweep out in the horizontal direction while maintaining a constant pressure on the contoured forming blocks.

Step 4: The pressurized fire hose sweeps around the radius of the contoured forming blocks.

Step 5: The pressurized fire hose sweeps down the vertical face of the contoured forming blocks. This is the final forming step and will be repeated until the full thickness of the laminate is achieved.

Step 6: The forming blocks are rotated for assembling the two formed laminates and preparing for cure. This step is performed after all plies of the laminate have been formed over the contoured forming blocks.

Step 7: The forming blocks are in the assembly position.

Step 8: The forming blocks are mechanically clamped together and transferred to the cure tool to be staged for the autoclave.

Among the below steps, the laminate is formed to the shape and contour of the forming blocks with the downward force from the fire hose through steps 2 to 5. The steps 6 to 8 are post forming steps and can be performed offline so they do not interrupt future forming processes on this automated forming equipment.

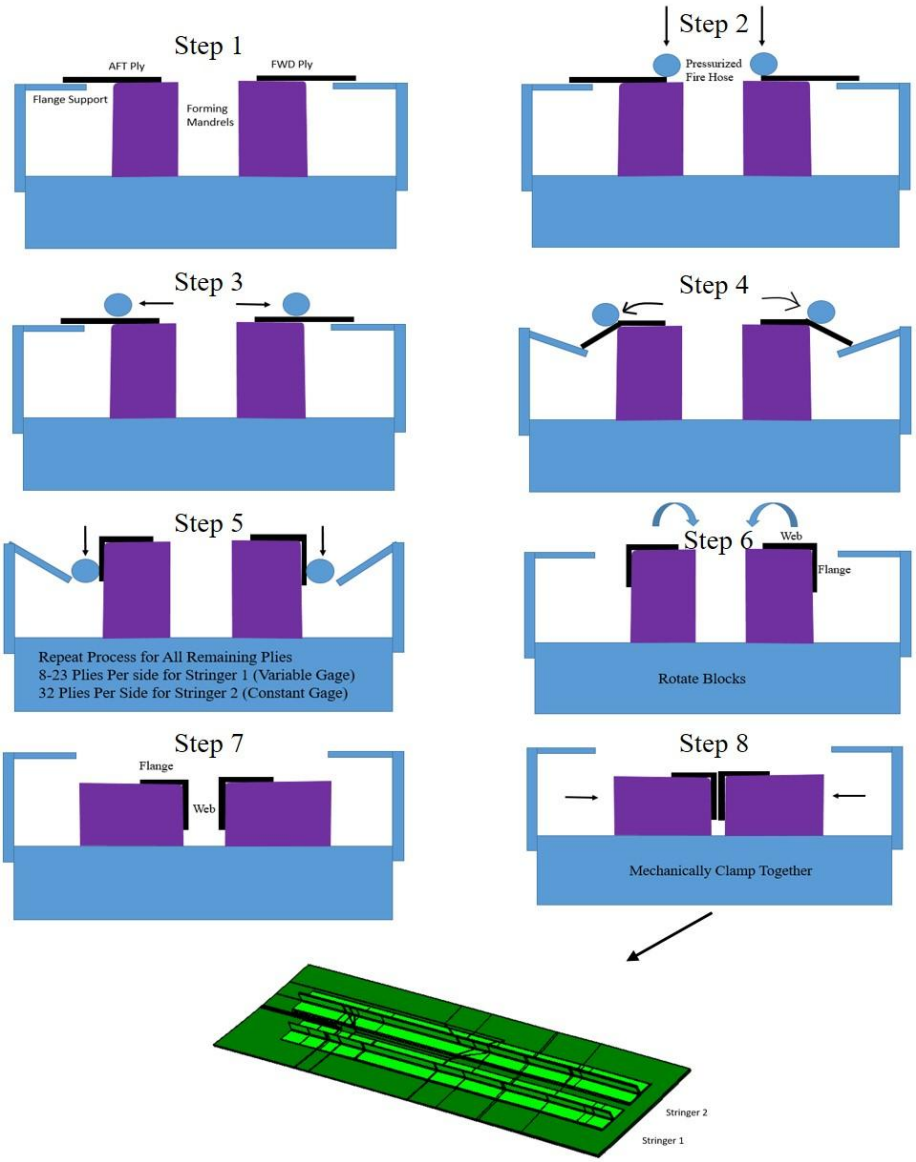

Figure 3. Forming process

2. PROBLEM DESCRIPTION

As mentioned before, this study focuses on the design of the end effector, which is a group of components that are responsible for touching/forming the composite laminate (Fig. 4) [5].

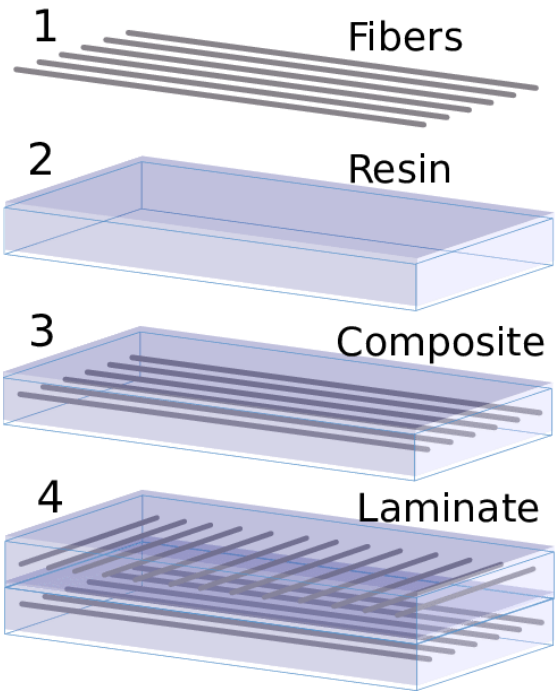

Figure 4. Schematic Picture of a Composite Laminate [5]

The end effector is made up of several 6061 aluminum pieces (actuated arm end plates, a rod end attach block, a base plate, a pivot rod end assembly, shaft blocks, and a hose plate assembly) and an inflatable fire hose. The inflatable fire hose is made from ethylene propylene diene monomer (EPDM) rubber that has an external fabric weave for strength and durability. A fire hose was chosen to act as the composite forming agent due to its high durability yet compliant structure.

Figure 5. A fire hose with a 4" (101.6) diameter

This study will be examining the non-linear analyses of the end effector inflated fire hose as well as the analyses of the aluminum plate and fittings that are part of the end effector assembly. The goals of the analysis will be computational analysis that will precede experimental trials.

3. AUTOMATED FORMING EQUIPMENT

A computer-aided design (CAD) model for the automated system was created using CATIA, as shown in Fig. 6. That figure also illustrates how this system can form two laminates simultaneously.

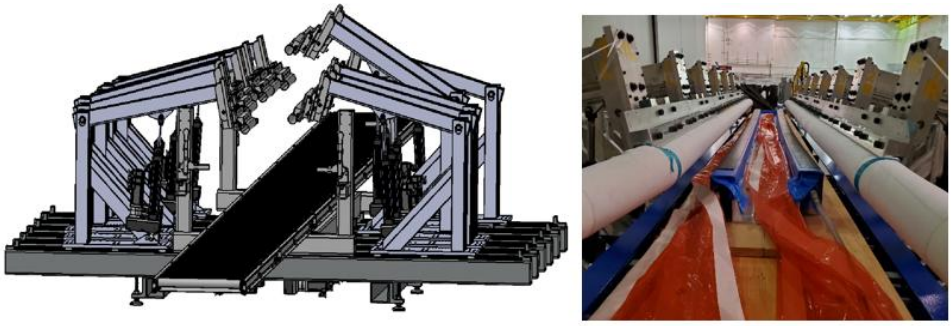

Figure 6. (L) A CAD model of the forming machine; (R) actual prototype of the forming machine

It can be seen from Fig. 6 that each end effector can move independently to one another but it is important to note that there will be a fire hose bridging the gap in between each of the end effector. The independent motions of individual end effectors make it possible to program the motions of the end effectors to move and independent of one another and form a laminate over different contours, joggles and asymmetric features.

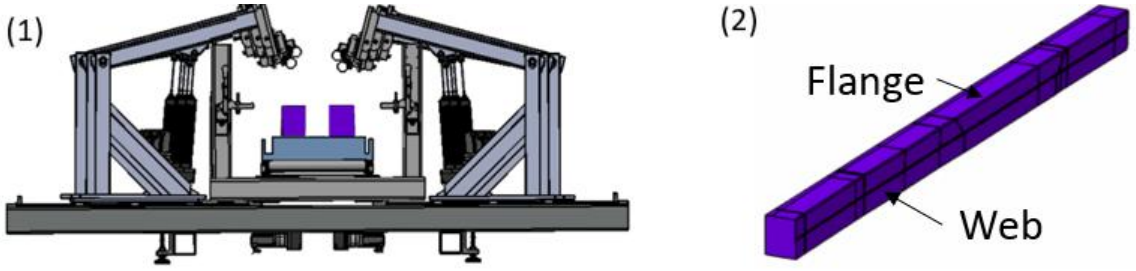

Figure 7. (L) The forming machine with forming mandrels; (R) and a contoured forming mandrel

The forming mandrels are approximately 135" (3.43 m) long and have a radius of curvature between 1000 in and 6000 in (25.4 m to 152.4 m) depending on the specific part that is being fabricated. The contoured forming mandrel is a tool that supports the laminate and has the features and contours of a specific commercial airplane wing stringer. This is the tooled surface the shapes the wing stringer. It has two surfaces that will contact the composite laminate. The top surface is the flange and the vertical surface is the web, and there is a 0.25 in (0.635 cm) radius that connects the two surfaces. There also are several joggles and steps on the surfaces of the mandrel. These features are the primary reasons that make it very difficult to create an automated forming equipment to form this specific composite structure because it is almost impossible to have such a machine roll over these surfaces without inducing any wrinkles on the laminate.

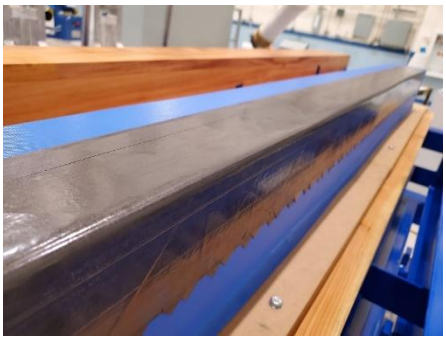

Figure 8. A composite laminate over a forming Mandrel

The machine will be forming at a very high speed as well. The primary reason that it needs to operate at a high speed is to prove the opportunity for this equipment in production by demonstrating faster cycle times to produce a wing stringer over alternative fabrication methods. The target speed is approximately 24 in/min (61 cm/min). For parts with highly complex geometries, this is an extremely fast speed but with increased speed usually comes the increased the chance of manufacturing poor quality laminates. Determining the proper end effector materials and assembly method will help ensure a high quality laminate at high speeds.

4. FINITE ELEMENT MODEL FOR END EFFECTOR

The end effector consists of a fire hose and the assembly components connecting it to an actuated arm. The fire hose is made up of EPDM rubber and nylon while the other components of the assembly are made up of aluminum. The fire hose has an EPDM internal bladder which expands with air pressure and a nylon exterior reinforced weave which protects the fire hose from bursting due to over pressurization. Key material properties are displayed in Table 1. For the fire hose, its material properties were estimated as a mixture of 90% Nylon and 10% EPDM. The end effector was simulated as an assembled system to see how the stresses react together. The material properties that were used are listed below.

Table 1. Material properties for FEA simulations [6, 7]

Material	Density (lb/in^3) / (kg/m^3)	Young's Modulus (KSI) / MPa	Poisson's Ratio
Aluminum	0.098 / 2712.631	1000 / 6894.760	0.334
Fire Hose	0.0392 / 1085.052	360.087 / 2482.712	0.4005

A general approach presented by Liu et al. [8-10] was followed to create the FEA models for the end effector and the fire hose, and all the simulations were completed in ABAQUS. As shown in Fig. 9, both models were meshed using C3D10 (a 10-node quadratic tetrahedron solid element). The two different element sizes 1.2 and 0.8 in (30.48 and 20.32 mm) were chosen for generating a variety of different meshes to evaluate the differences. This element size was determined after several element size sensitivity analysis to strike a balance between accuracy and efficiency of the FEA simulations [11-13]. Fig. 11 illustrates the loading and boundary conditions. Two different types of loading amplitudes were simulated to test if there were any differences in the results to protect for the loading to occur in different frequencies. The loading condition during the simulations is defined as follows: a pressure of 83 PSI (572 kPa) is applied on the hose contact area to generate a total force of 1000 lb (454 kg), which is exerted by the actuated arm moving the end effector down in the z-direction until the above pressures are reached. The hose contact area is 0.5 in (1.27 cm) wide and 24 in (61 cm) long. This is shown in a schematic in Fig. 10.

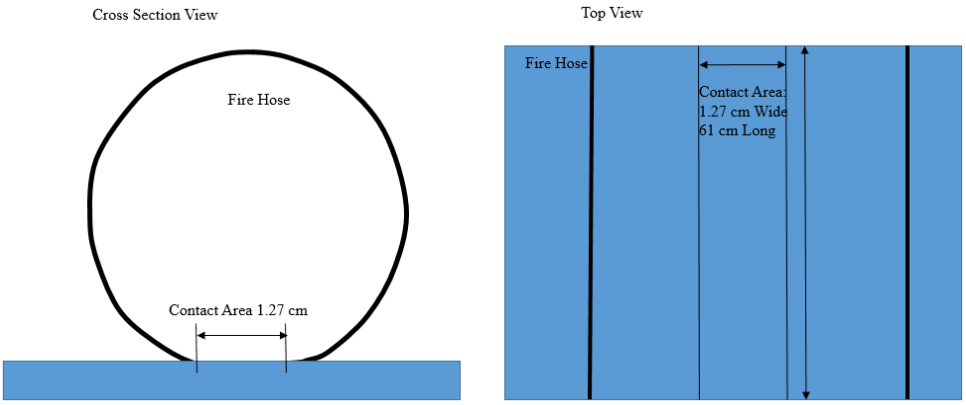

Figure 10. Schematic of contact area of fire hose

Simulation load condition: 1000 lb (454 kg), applied pressure over hose contact area:

$$\frac{1000lb}{0.5in \cdot 24in} = 83\ PSI$$

Which is 572 kPa over the hose contact area.

The simulation uses a tube for the fire hose, an exact 0.5 in (1.27 cm) contact area, and a clamped condition with the hose plate assembly; condition is no slip between the hose and hose plate, clamped condition between hose and hose plate assembly. The simulation is done using, first implicit model which is linear analysis then the results are compared with explicit dynamic analysis which is a nonlinear simulation. The assumption is that there is no slip between the fire hose and end effector. The tie condition was applied between the fire hose and end effector.

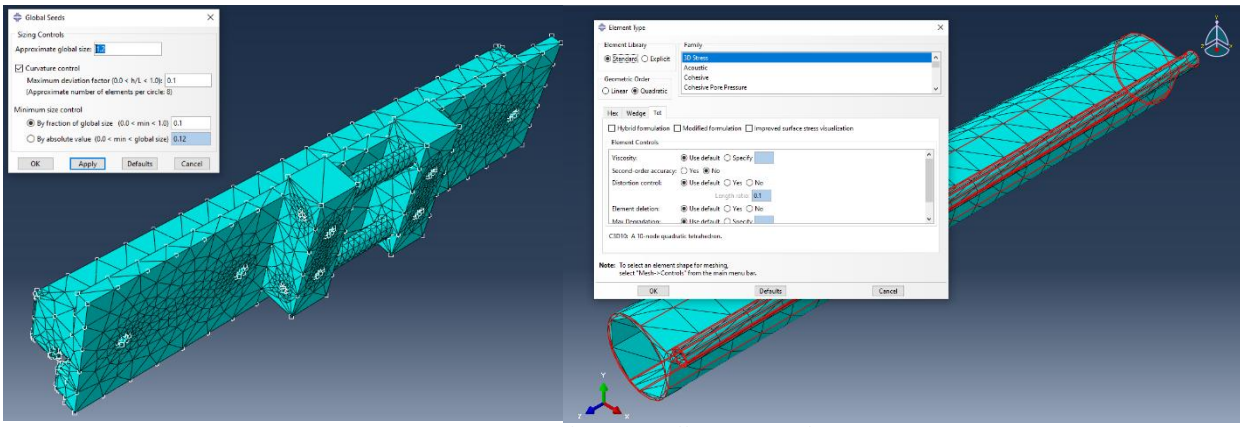

Figure 11. FEA models for the end effector and the fire hose

Load was applied from the bottom of the fire hose at 572 kPa and an internal fire hose pressure of 69 kPa was applied. Also, the right side of the end effector was fixed.

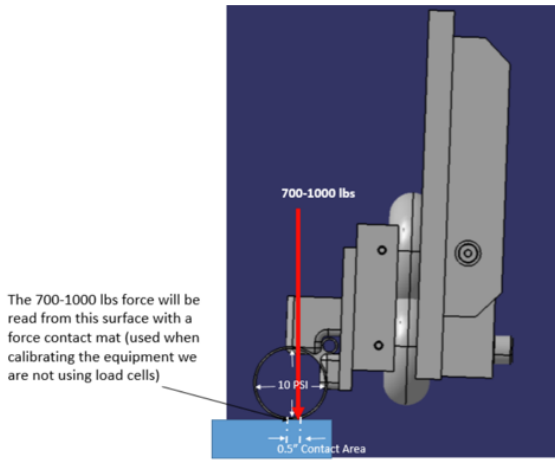

Figure 12. Loading conditions and boundary conditions

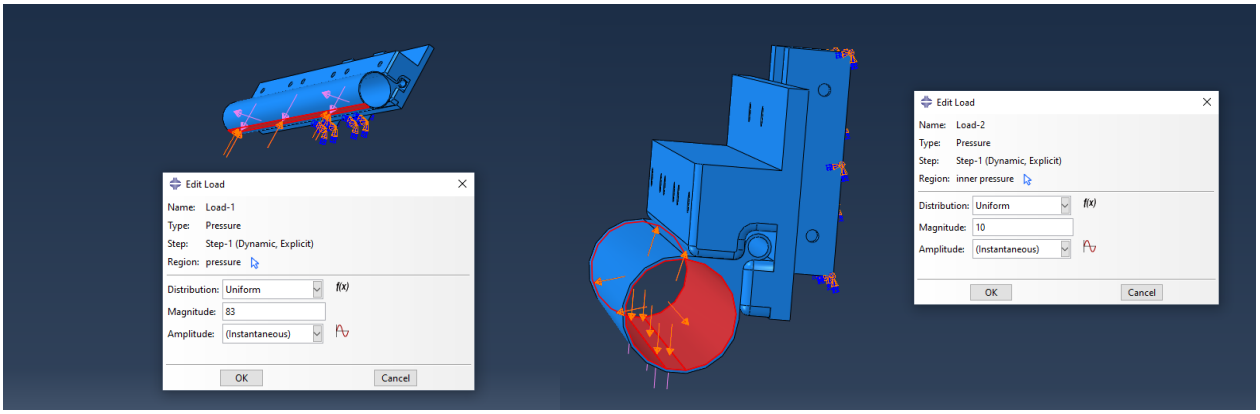

Figure 13. Applied loads and boundary conditions

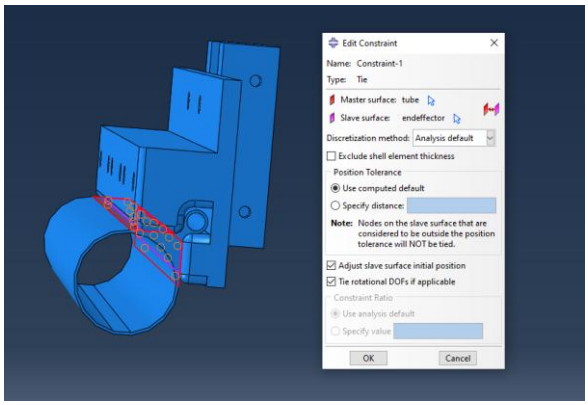

Figure 14. Tie condition between the fire hose and end effector

Key simulation parameters are listed in Table 2. The main purpose of this simulation is to see how the stress reacts together at different simulation approaches. Also, by decreasing mesh size, the optimal stress and deflection values were attempted to be solved.

Table 2. Set up and key parameters of FEA simulations

Cases	Analysis Type	Element Global Size (mm)	Time Period (sec)	Mass Scaling Factor	Load Amplitude
1	Implicit	30.48	1	N/A	Ramp
2	Implicit	20.32	1	N/A	Ramp
3	Explicit	20.32	0.09	No(1)	Smooth Step
4	Explicit	20.32	0.09	10	Smooth Step
5	Explicit	20.32	0.09	100	Smooth Step

5. RESULTS AND DISCUSSION

After completing the simulations, important results were extracted for each case and listed in table 3. As shown in that table, the maximum von Mises stress ranges from 3.29 to 13.51 kSI (22.47 to 93.15 MPa) and the maximum deflection varies from 0.06699 to 0.2968 inches (1.7 to 7.5 mm). Figs. 13 to 27 display the von Mises plots and deflection profiles obtained from each case.

The maximum von Mises stress occurs in Case 2; which has a global size of 20.32 mm. The higher observed stress is because of the smaller mesh size and the increased run time, which allowed the load to be applied evenly over one second. This allowed for a more accurate reading of stress. The lowest von Mises stress happens at Case 5; which had a global mesh size of 20.32 mm. The lower observed stress is primarily due to the increased mass scaling which scale the mass on a per step basis in a multistep analysis. An increase of the mass scaling increases the element-by-element stable time increment for an element set. This means that the elements were exposed to the load for a shorter amount of time. The smallest deflection of 1.701 mm happens at Case 1; which had a mesh size of 1.2 in (30.48 mm). However, when mesh size was decreased to 0.8 in (20.32 mm), the maximum deflection increased to 7.539 mm. Per mesh conversion approach, 7.539 mm value is considered a more accurate deflection value and

this implicit result is compared with the other explicit values for Cases 3, 4, and 5. Among them Cases 3 and 4 match well with implicit results. It can be assumed a mesh size of 1.2 in (30.48 mm) is too large and not able to observe all the deflection that is occurring since Cases 1 and 2 were identical in parameters except the size of the mesh and these resulted in the smallest and largest deflections.

Table 3. FEA simulation results

Cases	Max. Stress (Von-Mises) (MPa)	Max. Deflection (mm)
1	32.74	1.701
2	93.15	7.539
3	64.18	6.678
4	69.43	7.439
5	22.65	2.015

The below plot shows the max von Mises stress is 64.18 MPa at the shown location. This maximum stress happens inside the fire hose tube which is closed off to the end effector. This is expected since the pressure is being applied on the inner surfaces. The fire hose tensile strength is 137 MPa [14, 15], therefore it is within the range. Also, the highest stress is located at a stress concentration area, so it is safe to assume the fire hose is within an acceptable range of its maximum tensile strength. Case 4 max stress is a little higher than other explicit simulations, however the deflection is very close to case 2 and 3. Case 1 deflection is lowest.

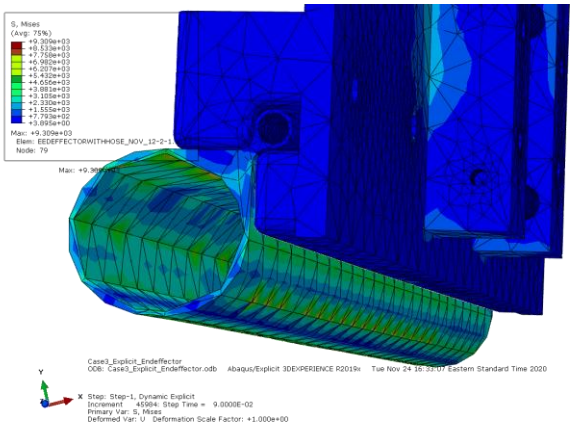

Figure 15: Max Stress at Case 3

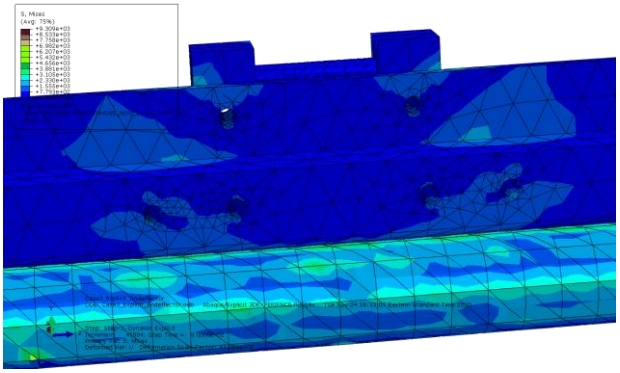

Figure 16: Von Mises Stress at Case 4

By looking at the different figures the majority of the end effector stress area is under 20 MPa, which is well under the fire hose and aluminum ultimate tensile strengths of 137 MPa and 310 MPa respectively. The below plot shows a max deflection of 6.678 mm in the shown location. The largest deflection happens at the contact area, which was anticipated because the contact area surface of the fire hose that is being pressed with 454 kg would indeed have the largest defection. This is not expected to be an issue while operating as it appears to be a reasonable amount of deflection and all the stresses are within the limits of the materials.

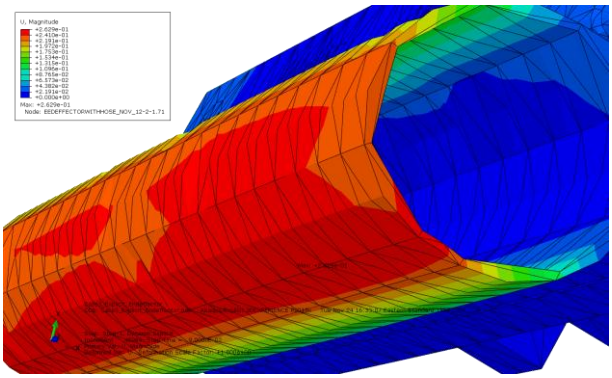

Figure 17: Max Deflection at Case 3.

Figure 17 shows case 3 which is representative of the explicit simulations. For Cases 3 and 4, the kinetic energies are relatively small compared to internal energies. Therefore Cases 3 and 4 simulations are considered close to quasi-static condition simulation, whereas Case 5 shows kinetic energy is higher by a significant amount, so it is not considered quasi-static simulation.

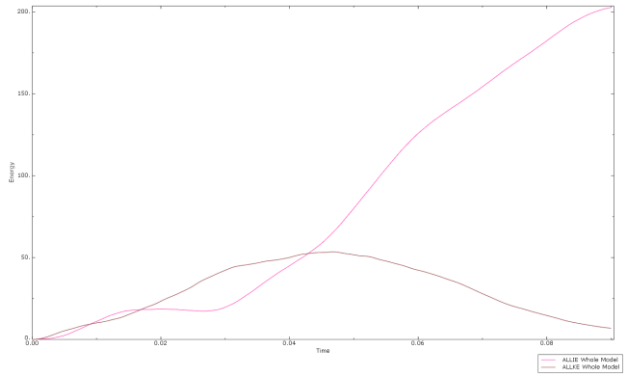

Figure 18: Case 4 Comparison of Internal energy and Kinetic energy

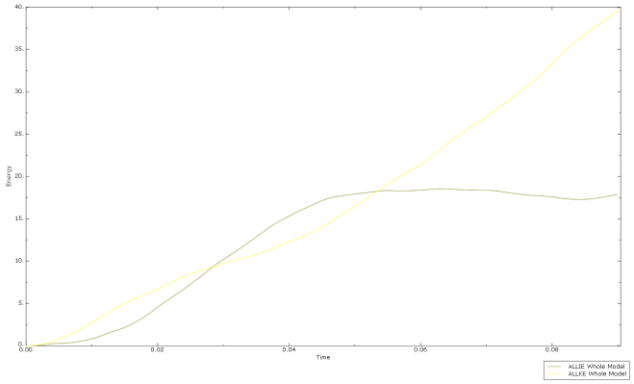

Figure 19: Case 5 Comparison of Internal energy and Kinetic energy

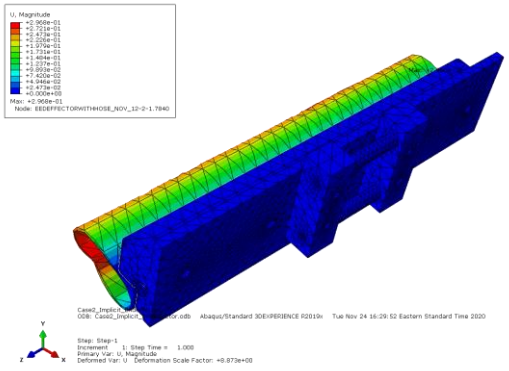

Figure 23: Case 2 Deflection Plot

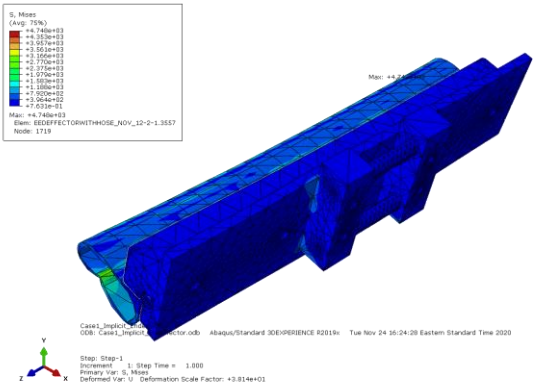

Figure 20: Case 1 Von-Mises Plot

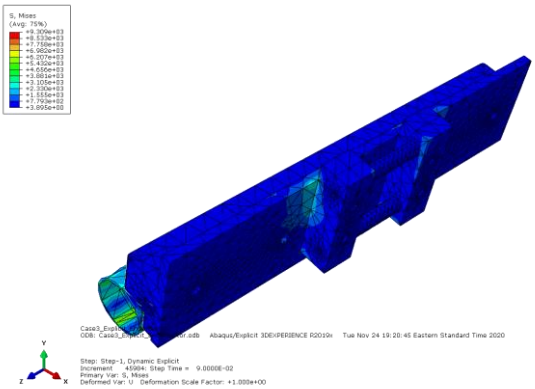

Figure 24: Case 3 Von-Mises Plot

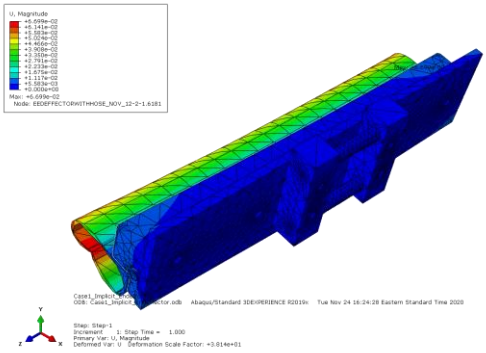

Figure 21: Case 1 Deflection Plot

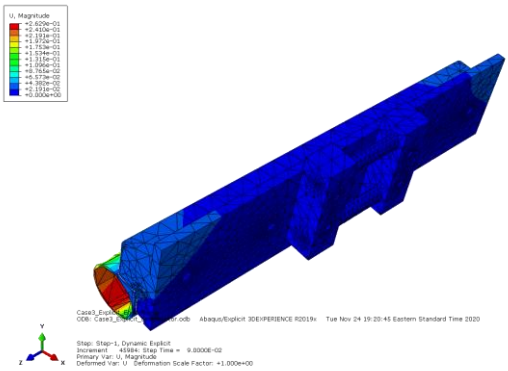

Figure 25: Case 3 Deflection

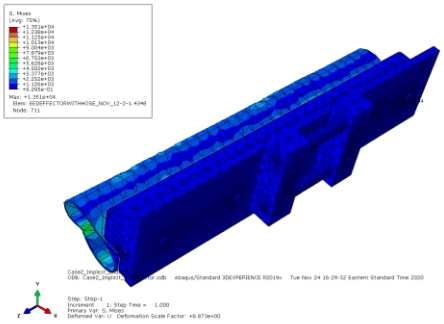

Figure 22: Case 2 Von-Mises Plot

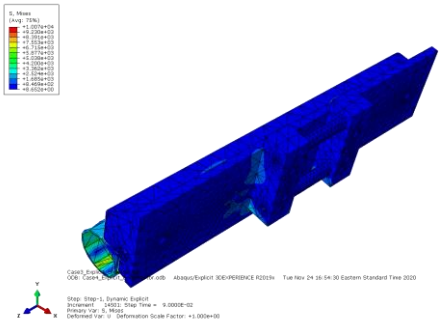

Figure 26: Case 4 Von-Mises Plot

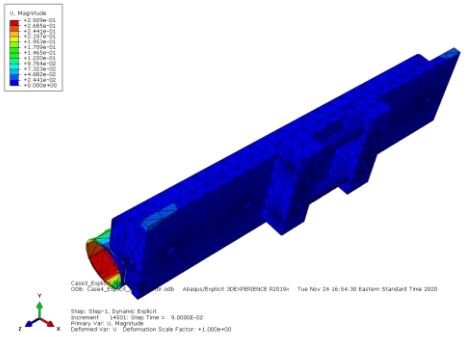

Figure 27: Case 4 Deflection Plot

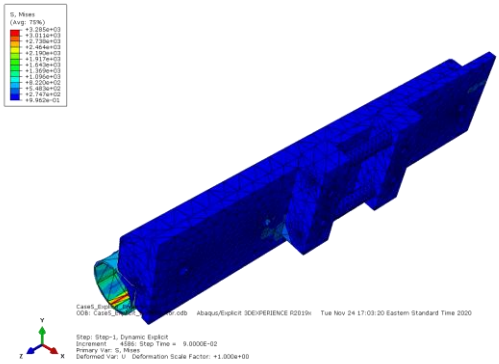

Figure 28: Case 5 Von-Mises Plot

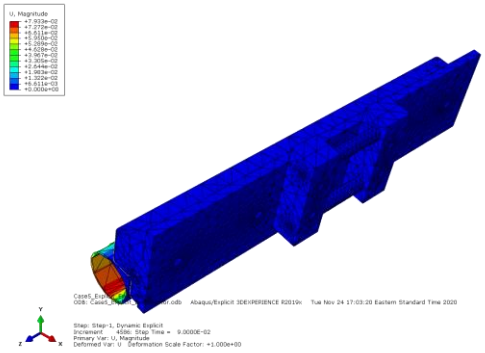

Figure 29: Case 5 Deflection Plot

6. CONCLUSIONS

A computational approach using finite element analysis (FEA) was used to examine the end effector materials and the assembly to confirm that they are robust enough to withstand the internal and external stresses and forces without failure or permanent deformation of the end effector materials, forces which are created from the pressurized fire hose and reactive force on the fire hose from the pressure being applied to an independent tool. From all the simulations it looks like the fire hose will undergo a sizable amount of deformation and stress. The aluminum is much lower on deformation scale and with stress around 20.684 MPa, it is not anticipated to be any issue in operation. Although the deformation and stress that the fire hose undergoes is not negligible, it should be low enough to proceed to test in real conditions. Especially considering the fact that this end effector will be tied to 5 additional end effectors which will help distribute the stress a bit. The desired effect of using a fire hose to be rigid yet forgiving seems to be confirmed with this simulation. The fire hose will be rigid and stiff when pressing and compacting the composite laminate but also forgiving so it may be possible to contour over curvatures and joggles. Whether or not this design will produce high quality composite materials is to be determined but this simulation has proven that it may be feasible.

7. REFERENCES

[1] Grant, C., "Automated processes for composite aircraft structure", *Industrial Robot*, Vol. 33 No. 2, 2006, 117-121.

[2] Willden, K.S., Van West, B.P., Harris, C.G., "Forming method for composites", US Patent No. 8,142,181, 2012.

[3] Reeves, J.A., Carlson, L.C., Pham, K.M., et. al., "Methods for forming a composite blade stiffener and facilitating application of barely visible impact damage treatments", US Patent No 10,377,091, 2019

[4] Talreja, Ramesh, "Manufacturing defects in composites and their effects on performance", *Polymer Composites in the Aerospace Industry*, 2015, 99-113

[5] Jareteg, Cornelia & Wärmefjord, Kristina & Cromvik, Christoffer & Söderberg, Rikard & Lindkvist, Lars & Carlson, Johan & Larsson, Stig & Edelvik, Fredrik. (2016). "Geometry Assurance Integrating Process Variation With Simulation of Spring-In for Composite Parts and Assemblies". *Journal of Computing and Information Science in Engineering*. 16. 10.1115/1.4033726.

[6] "Aluminum Mechanical Properties", *ASM Aerospace Specifications Metals Inc.*, http://asm.matweb.com/search/SpecificMaterial.asp?bassnum=MA6061T6. Accessed from 24 Aug 2021

[7] "Marco Rubber Compound # E1121 90 Durometer, Black, EPDM for Geothermal Applications Technical Datasheet" *Marco Rubber*, https://www.marcorubber.com/downloads/Marco-Material-Datasheet-E1121.pdf. Accessed from 24 Aug 2021

[8] Y.-C. Liu and Q.-K. Wang, "Computational study of strengthening effects of stiffeners on regular and arbitrarily stiffened plates", *Thin-Walled Structures*, 59, 2012, 78-86.

[9] Y.-C. Liu and M.L. Day, "Experimental analysis and computer simulation of automotive bumper system under impact conditions", *International Journal of Computational Methods in Engineering Science and Mechanics*, 9(1), 2008, 51-59.

[10] Y.-C. Liu, "Design enhancement of thin-walled steel beams with improved stiffness and reduced weight", *International Journal of Design Engineering*, 1(2), 2008, 149-165.

[11] Y.-C. Liu and G.A. Glass, "Effects of mesh density on finite element analysis", SAE Technical Paper 2013-01-1375, 2013.

[12] Y.-C. Liu, "ANSYS and LS-DYNA used for structural analysis", *International Journal of Computational Aided Engineering and Technology*, 1(1), 2008, 31-44.

[13] "Voloknohim Nylon Fiber 0.68 Tex", *MatWeb Material Property Data*, http://www.matweb.com/search/DataSheet.aspx?MatGUID=675b77f996b142f59e4cb60d69d64872&ckck=1. Accessed from 24 Aug 2021

[14] "High Tensile Strength Flexible Lightweight PU Fire Hose", *Quanzhou Winner Fire Fighting Equipment Co. Ltd.*, http://www.winnerfirehose.com/high-tensile-strength-flexible-lightweight-pu-fire-hose_p151.html. Accessed from 24 Aug 2021

International Journal of Science and Engineering Applications
Volume 10-Issue 11, 163 - 173, 2021, ISSN:- 2319 - 7560

Modelling of Electric Grid to Enhance Generated Power Evacuation

Donald Eloebhose
Dept. Electrical/Electronic Engineering,
University of Port Harcourt,
Rivers State, Nigeria

Nelson Ogbogu
Dept. Electrical/Electronic Engineering,
University of Port Harcourt,
Rivers State, Nigeria

Abstract: The study of evacuation of power from the power plants in Rivers State Nigeria, connecting to the 330kV transmission network of the Transmission Company of Nigeria (TCN). The Power World Simulator Educational version was used in the modelling and simulation of the electric power grid. The study of load flow analysis, short circuit, transient and N-1 contingency analysis and their effect on the 330 kV/132kV transmission bus connected to the existing power plants in Rivers State Nigeria namely; Rivers IPP (180MW), Afam III (265.6MW), Afam IV & V (351.00 MW) and Afam VI G. S (650.00 MW) was carried out. From the short circuit study, it is observed that when a bus is faulted with a 3-phase fault, the three-phase voltages of the system drastically become zero in all the phases. The other buses of the network experience an increase in voltage and all the buses fed have the same effect as the bus under fault, though the effect is felt more on the buses. However, with the introduction of substation splitting at Afam III and ongoing Afam IV substations, the short circuit level will be reduced by 15%; leading to improvement in the overall system stability.

Keywords- Power World Simulator, Afam, Short circuit analysis, load flow analysis, contingency analysis, transient analysis.

1. INTRODUCTION

The requirement for electric power is constantly increasing, for socio-economic growth in nations of the world, a steady electricity supply is key. The electricity condition in Nigeria currently is poor and nothing to write home about, study shows that, inadequate management of plants and old machines are instrumental to the poor electricity condition in the country [1]. The poor power in Nigeria was largely due to the poor transmission ability of the national grids system and the poor power of the national grid generating capacity of the nation's generating stations among others [2]. Nigeria's major means of generating electricity include thermal, hydro and gas generating stations all distributed over the nation. Nigeria, with its diverse array of renewable and non-renewable energy resources can alleviate the electricity generation crisis. For instance, the country has natural gas reserves of 185 trillion cubic feet, coal reserves of 2.75 billion tons, and crude oil reserves of 35 billion barrels [3]. The above non-renewable energy reserve is sufficient to meet Sub-Saharan Africa's electricity generation demand for many decades [1]. Despite having ample capacity to generate enough energy for its people, Nigeria continues to struggle to meet its citizens' energy needs. Considering the significance of infrastructural facilities and the use of energy in Nigeria, economic development seems to have been sluggish given the absence of power supply.

This is likely to have contributed to the country's slow growth rate, this is most likely a reflection of the country's poor infrastructure growth and why, despite its abundant natural resources, Nigeria is one of the world's poorest economies [4]. The demand for this essential utility is directly proportional to population size. As the population size increases the demand also increases resulting in a corresponding increase in the burden of existing transmission systems, that is, increase in the population size over time will affect the existing transmission lines to be overloaded beyond their designed ratings with a consequent reduction in electrical power transmission quality and in extreme cases; there is total power outage [5]. The key factors behind this situation are the lack of electricity transmission due to the lack of state-of-the-art facilities, the intrinsic deficiency of the current electricity transport system and, of course, the insufficient investment in the power generation sector. This means that the nearly 200 million people in society will find the supply of electricity and the mission of ardor, translating into an energy-deficient society with 121 KWh per capita, 50 times less than the average country in Europe with 10% of the population of Nigeria [6]. There is a need to build more and more powerful electricity generating stations to meet the growing demand, however, this generated power is ultimately distributed to customers. The electrical power grid network is made up of a generating station, sub-station, transmission and distribution lines.

This study uses Power World Simulator Educational version to analyze load flow, short circuit, transient and N-1 contingency analysis and their effect on the 330 kV/132kV transmission bus connected to the existing generators in Rivers State Nigeria namely; Rivers IPP (180MW), Afam III (265.6MW), Afam IV & V (351.00 MW) and Afam VI G. S (650.00 MW).

2. LITERATURE REVIEW

Power evacuation is a vital feature that enables generated power to be immediately evacuated for transmission and distribution from the generator to the grid. Over the years, power evacuation experiments have been performed primarily for the introduction of new generators into the grid system. Several studies were carried out by [7-12]. Such as the design of 132kV power evacuation system at Bawktlang substation in Mizoram, India [7]. Optimal analysis of power evacuation of Tiga hydro generator in Kano State [8]; this study did not take into account the fault contribution of the generators to the current network, but carried out comprehensive studies on load flow, Synopsis of maximum control evacuation from the generator to the power grid in Madhya Pradesh. The studies conducted by [7] and [9] do not include all the basic technical details essential for optimizing the smooth evacuation of an

existing power grid from a new generator. Modelling of an electric Grid for the Evacuation of a new generator carried out by [10]. The introduction of a new generator into a current electricity grid alters the behavior of the power grid into which it is introduced. This study focuses on the performing studies to improve electric power evacuation on an existing power plant. To achieve these serval studies will be performed such as load flow studies [13-17], fault current and the use network bus splitting for reduction of 3-phase fault current [18-19], transient analysis [20-21] and N-1 contingency [22-23]. And research has shown that electricity consumption will continue to increase in Nigeria [24]. Thus, there is need to build more power generating stations and most importantly evacuate all the generated power to the grid system.

In this study, analytical software for the power system was used. This study aims to model an electric power grid of river state generation plants and to certain defined studies on the case study by eliminating one generating plant. Using Power World Software, the impact of the removed generator the entire system was studied.

3. MATERIALS AND METHOD

The transmission network of 330 kV/132kV transmission bus connected to the existing generators in Rivers State Nigeria namely; Rivers IPP (180MW), Afam III (265.6MW), Afam IV & V (351.00 MW) and Afam VI G. S (650.00 MW) was modelled using power world simulation software v21.1

3.1 Load Flow Modelling

In this power system evacuation study, buses are considered for modelling see figure 1.

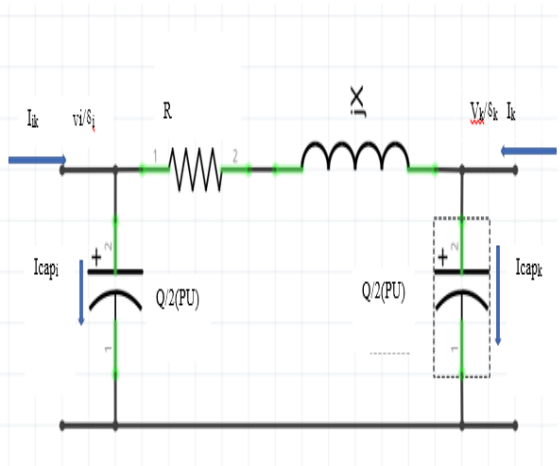

Figure 1: A two-bus power system

$$V_i = |V_i|e^{j\delta_i} = V_i(\cos\delta_i + \text{jsin}\,\delta_i) \quad (1)$$

$$Y_{ik} = |V_{ik}|e^{j\delta_{ik}} = V_i(\cos\delta_{ik} + \text{jsin}\,\delta_{ik}) \quad (2)$$

2

Where,

P means Active Power (MW),

Q means Reactive Power (MVAR),

V means the Magnitude of Bus Voltage (kV),

δ means Bus Voltage Angle (Degree).

Therefore, Complex power is:

$$S_i = P_i + jQ_i = V_i I_i \quad (3)$$

Consider generator and load

$$P_i = P_{Gi} - P_{Li} = Re[V_i I_i^*] \quad (4)$$

$$P_i = P_{Gi} - P_{Li} = Im[V_i I_i^*] \quad (5)$$

Then, the expression for bus is:

$$I_{bus} = Y_{bus} V_{bus} \quad (6)$$

A new arrangement for equations (3), (4) and (5) gives (7), (8) and (9). While the polar form gives (10), (11) and (12)

$$I_{bus} = \frac{P_i + jQ_i}{V_i^*} = Y_{ii}V_i + \sum_{k=1}^{n} y_{ik}V_k \quad (7)$$

$$V_i = \frac{1}{Y_{ii}}\left[\frac{P_i - jQ_i}{V_i^*} - \sum_{k=1}^{n} Y_{ik}V_k\right] \quad (8)$$

$$P_i + jQ_i = V_i \sum_{k=1}^{n} Y_{ik}V_k \quad (9)$$

$$P_i + jQ_i = V_i \sum_{k=1}^{n} |Y_{ik}V_k V_i| e^{j(\delta_i - \delta_k - \theta_{ik})} \quad (10)$$

$$P_i = \sum_{k=1}^{n} |Y_{ik}V_k V_i| \cos(\delta_i - \delta_k - \theta_{ik}) \quad (11)$$

$$Q_i = \sum_{k=1}^{n} |Y_{ik}V_k V_i| \sin(\delta_i - \delta_k - \theta_{ik}) \quad (12)$$

Where,

$$i = 1,2,\ldots,n; \qquad i \neq slack\ bus$$

3.2 Short Circuit Modelling

For short circuit research, the IEC 60909is applied. In the equations, more is illustrated. Using the symmetrical elements, compute the original short-circuit current. After the rms I_k is known, it is possible to measure others.

$$I_k'' = \frac{cV_n}{\sqrt{3}Z_k} \quad (13)$$

$$Z_k = |R_k + jX_R| \quad (14)$$

Where,

Vn = nominal voltage, C = voltage factor

At the fault spot, (V), Z_k = impedance. R_k and X_k =resistances and reactance respectively. One can calculate the ratio using the corresponding R and Positive sequence impedance at the fault site.

$$\cdot \frac{X}{R} = \frac{X_k}{R_k} \quad (15)$$

Ip= peak current given as
Where,

$E_i' = |E_i'|\angle\delta_i$ and $|Y_{ij}| = |Y_{ij}|\angle\theta_{ij}$ and Y_{ij} is the ij[th]

$$I_p = 1.15\beta\, X\, \sqrt{2I_k''} \quad (16)$$

Where β is expressed as,

$$\beta = 1.02\ X\ 0.9e^{\frac{3}{X/R}} \quad (17)$$

3.3 Transient Stability Analysis Model

The analysis of transient stability begins by solving the initial flow of load and initial flow of the bus. About voltages. Before disturbance, the following equation 3.17 computes the machine currents.

$$I_i = \frac{S_i^*}{V_i^*} \quad (18)$$

$$i = 1,2,\dots,m$$

Here, Number of generators, generator terminal voltage, and generator complex power

$$E_i' = V_i + jX_d' I_i \quad (19)$$

$$y_{i0} = \frac{S_i^*}{|V_i^2|} \quad (20)$$

For the electircal power is computed as

$$P_{ei} = \sum_{j=1}^{m} |E_i'| |E_j'| |Y_{ij}| \cos(\theta_{ij} - \delta_i + \delta_j) \quad (21)$$

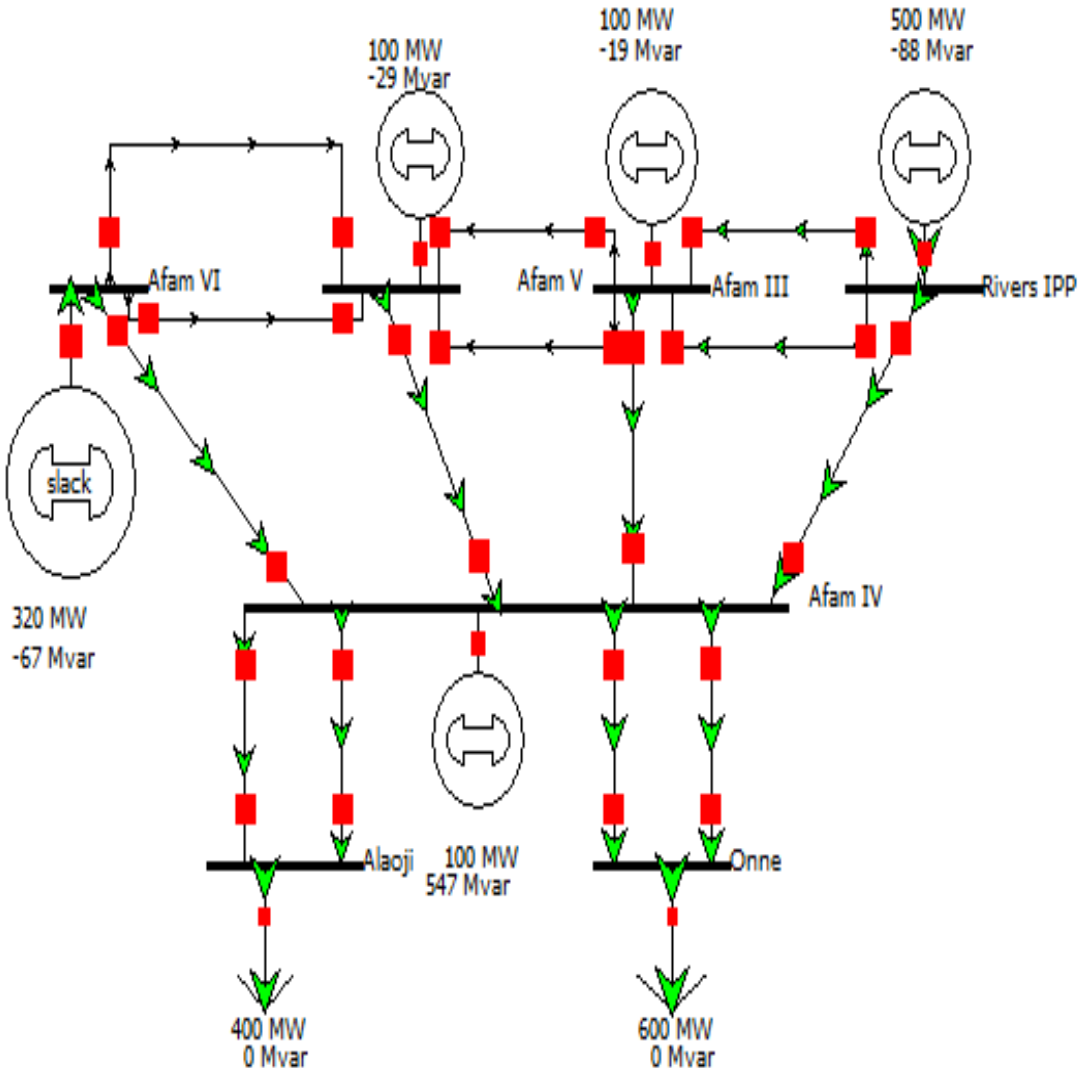

Figure 2. The Power world simulator model of the TCN 330/132 KV Network

4. RESULTS AND DISCUSSION

4.1 Results of Load Flow Studies

In addition, the Analysis of power flow in the entire 132KV of the River State Generators to understudy the voltage profile in the power plant network was studied. In the cases analyzed, Table 1 presents the voltage profile in power plant buses is within reasonable limits (1.0 PU). See illustration

4.2 The Results of Equipment Loading

There are no overloaded components in the study case; however, when the system is loaded to 150, percent of the power generating capability of the entire system, its entire network blacks out due to the network overloading, see Figure 3. In this case, the incorporation of a new generation station will resolve the issue.

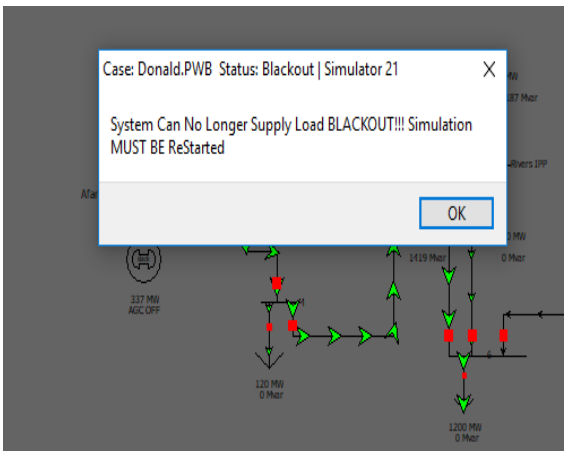

Figure 3: Result of Equipment Loading

4.3 The Results of Short Circuit Studies

This work considers 3- phase fault for analysis of short circuit to ascertain fault voltages and at the different current level generator inside the interconnected structure, buses to check Adequacy of Switchgear ratings. This was done by applying a fault of three phase on all the 132 kV bus bars in the system undergoing analysis. When a bus is faulted with a 3-phase fault, the three-phase voltages of the system drastically become zero in all the phases. The other buses of the network experience an increase in voltage and all the buses fed have the same effect as the bus under fault, though the effect is felt more on the buses.

Table 1: Analysis of power flow of the network under study

Number	Name	Area Name	Nom KV	PU Volt	Volt (kV)	Angle (Deg)
1	Afam VI	1	132.00	1.0000	132.00	0.00
2	Afam V	1	132.00	1.0000	132.00	-4.15
3	Afam III	1	132.00	1.0000	132.00	-4.20
4	Rivers IPP	1	132.00	1.0000	132.00	-0.15
5	Afam IV	1	132.00	0.77592	102.421	-16.5
6	Alaoji	1	132.00	0.68403	90.293	-34.11
7	Onne	1	132.00	0.57977	76.530	-46.30

Table 2: 3-phase Fault Afam VI

Number	Name	Phase Volt A	Phase Volt B	Phase Volt C	
1	Afam VI	0	0	0	
2	Afam V	0.1773	0.1773	0.1773	
3	Afam III	0.27426	0.27426	0.27426	
4	Rivers IPP	0.34973	0.34973	0.34973	
5	Afam IV	0.271	0.271	0.271	
6	Alaoji	0.25664	0.25664	0.25664	
7	Onne	0.24405	0.24405	0.24405	

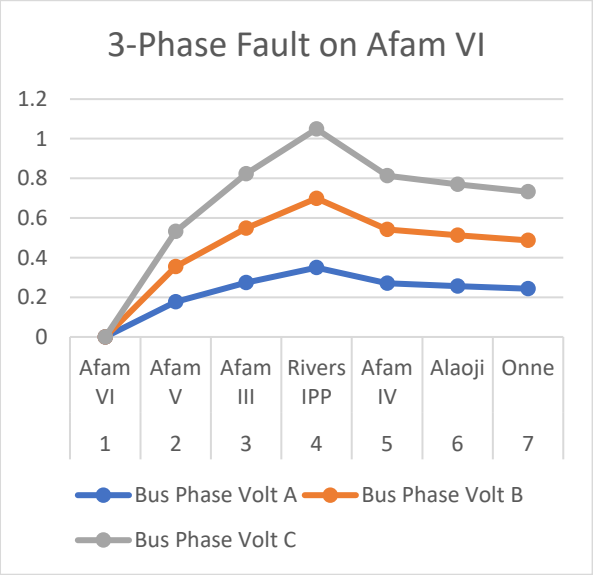

Figure 4: 3-Phase Fault on Afam VI

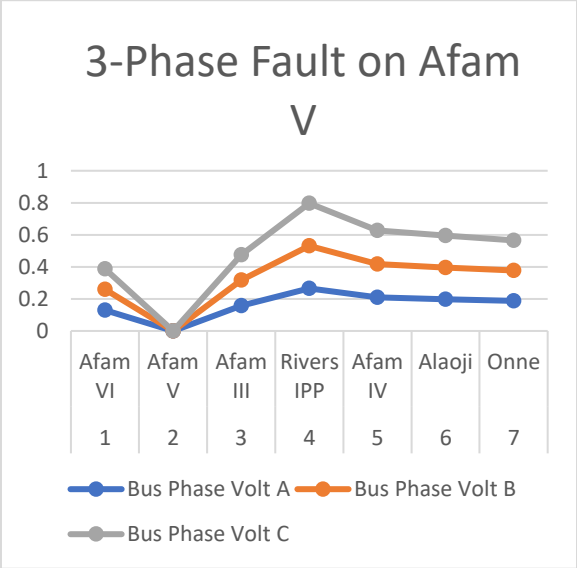

Figure 5: 3-Phase Fault on Afam V

Table 3: 3-Phase Fault on Afam V

Number	Name	Phase Volt A	Phase Volt B	Phase Volt C
1	Afam VI	0.12944	0.12944	0.12944
2	Afam V	0	0	0
3	Afam III	0.15845	0.15845	0.15845
4	Rivers IPP	0.26558	0.26558	0.26558
5	Afam IV	0.20927	0.20927	0.20927
6	Alaoji	0.19818	0.19818	0.19818
7	Onne	0.18846	0.18846	0.18846

Table 4: 3-Phase Fault on Afam III

Number	Name	Phase Volt A	Phase Volt B	Phase Volt C
1	Afam VI	0.21533	0.21533	0.21533
2	Afam V	0.14004	0.14004	0.14004
3	Afam III	0	0	0
4	Rivers IPP	0.1615	0.1615	0.1615
5	Afam IV	0.20532	0.20532	0.20532
6	Alaoji	0.19444	0.19444	0.19444

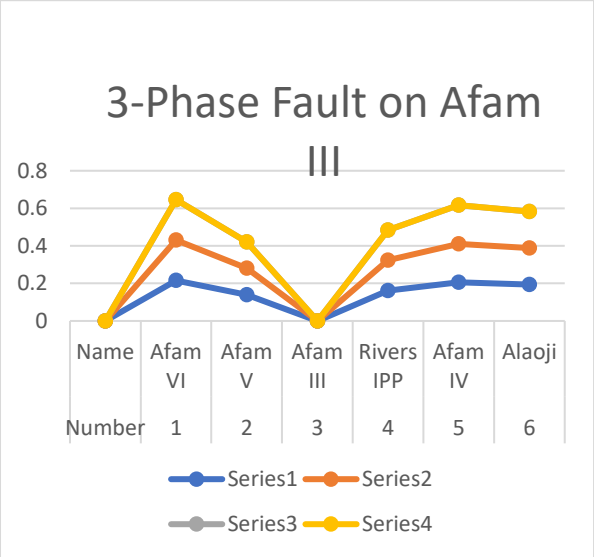

Figure 6: 3-Phase Fault on Afam III

Table 5: 3-Phase Fault on Rivers IPP

Number	Name	Phase Volt A	Phase Volt B	Phase Volt C
1	Afam VI	0.28949	0.28949	0.28949
2	Afam V	0.24397	0.24397	0.24397
3	Afam III	0.16408	0.16408	0.16408
4	Rivers IPP	0	0	0
5	Afam IV	0.26155	0.26155	0.26155
6	Alaoji	0.24769	0.24769	0.24769
7	Onne	0.23554	0.23554	0.23554

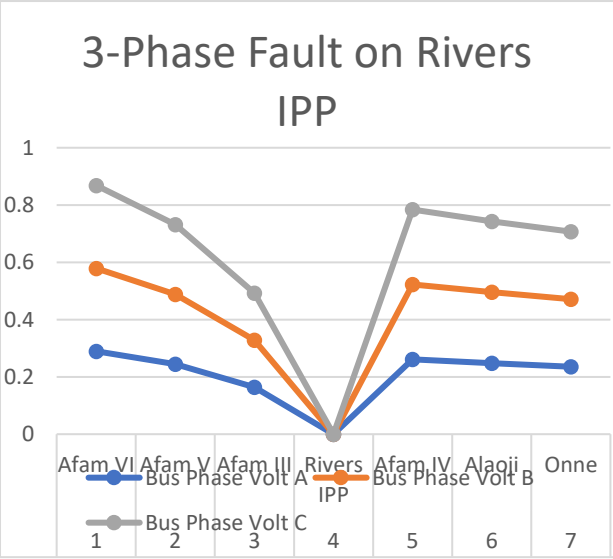

Figure 7: 3-Phase Fault on Rivers IPP

Table 6: 3-phase Fault on Afam IV

Number	Name	Phase Volt A	Phase Volt B	Phase Volt C
1	Afam VI	0.19568	0.19568	0.19568
2	Afam V	0.16803	0.16803	0.16803
3	Afam III	0.18377	0.18377	0.18377
4	Rivers IPP	0.25264	0.25264	0.25264
5	Afam IV	0	0	0
6	Alaoji	0	0	0
7	Onne	0	0	0

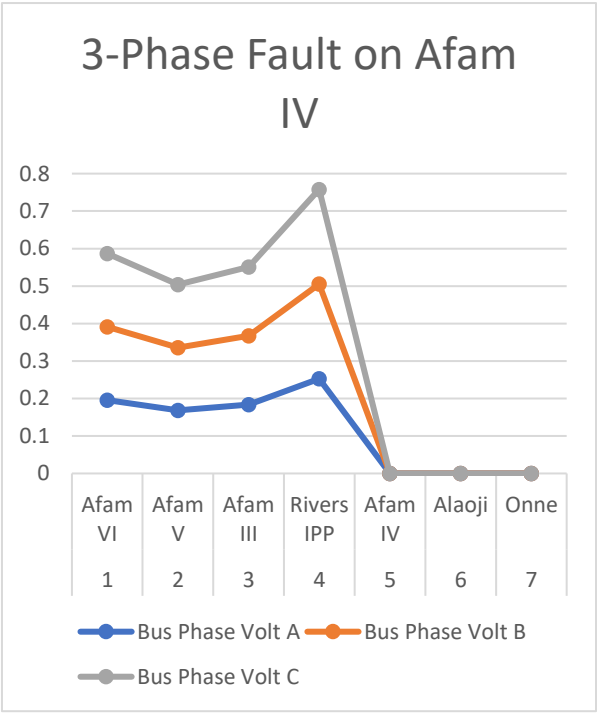

Figure 8: 3-Phase Fault on Afam IV

4.4 The Results of Reduction of Fault Current through Substation Splitting.

Substation splitting was performed in Afam V and 132 kV generators were opened in Afam III in attempt to lessen the short circuit current throughout the system, and new fault current levels in the network were identified throughout the system buses. The percentage reduction of the default current is seen in Table 7 and Figure 9 owing to the removed generator.

Table 7 Fault Current when Afam V and III are shutdown

Number	Name	Fault Current Amps	Current before Fault Amps	Current after Split
1	Afam V	4095	4202	4088
2	Afam IV	4535	4202	3947
3	Afam III	4535	4202	4088
4	Afam VI	5378	4202	4980
5	Rivers IPP	4202	4202	3947

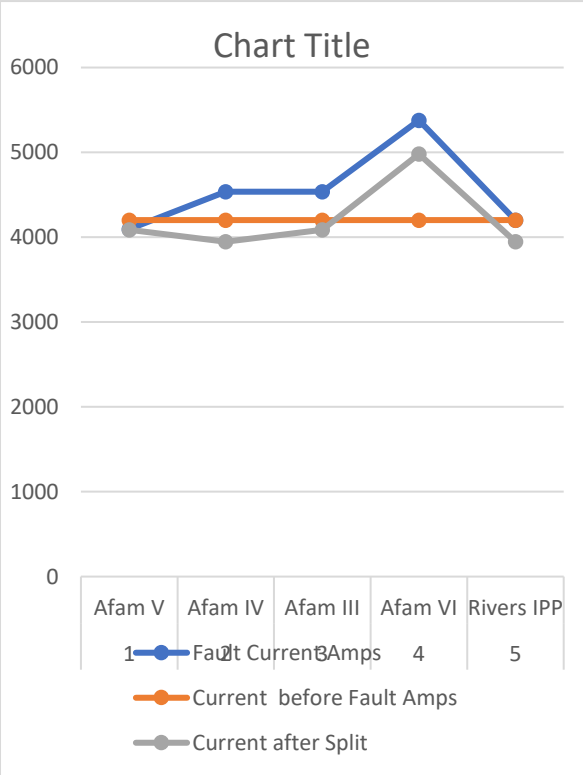

Figure 9: Fault current when Afam III and V are shutdown

4.5 The Results of Transient Stability Studies

As the Afam IV bus 132 kV faulted with a three phase faults for 150 ms, this is simulated by the insertion of a shunt with 0.00001 p.u reactance at the power station. To monitor the effectiveness of the multiple generators in order to clear the fault duration, the shunt is originally turned out, then turned at 2.0 seconds following the study begins, and cleared after 10 iterations.

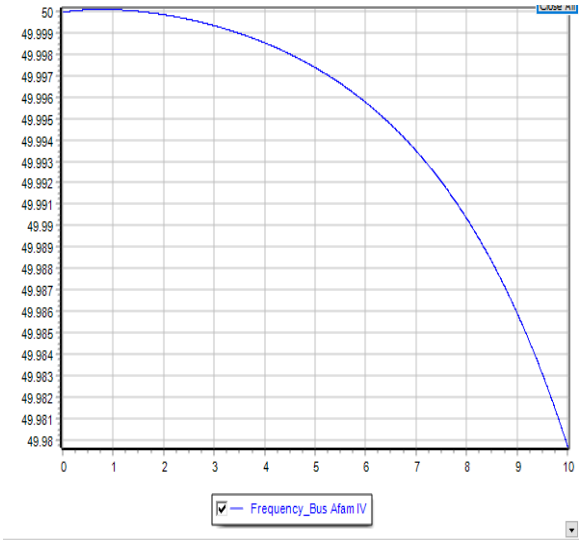

Figure 10: Afam IV 132 kV bus was faulted with 3-phase to ground fault for 150 ms.

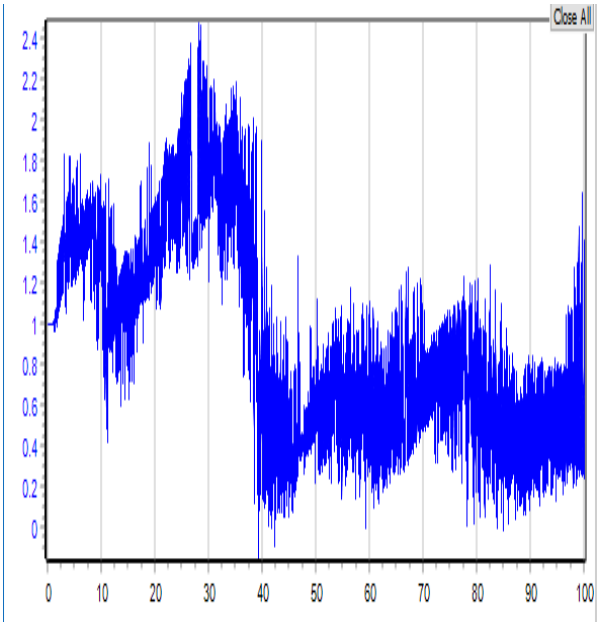

Figure 11: Afam IV 132 kV bus was faulted with 3-phase to ground fault for 150 ms.

4.6 The Results of Bus and Rotor Angle

The curves of the angle Figure 9 show how the whole system is maintained for various generators in the system. The angle differences between the different units are minimal. It's also worth noting that there's a uniform oscillation of the angles of bus voltage to a new location within the proper limit, thus testing the system's stability. Other units' angular differences were not too distinct in the process from one another. The rate of many other units, in particular, is fairly consistent with reduced oscillation.

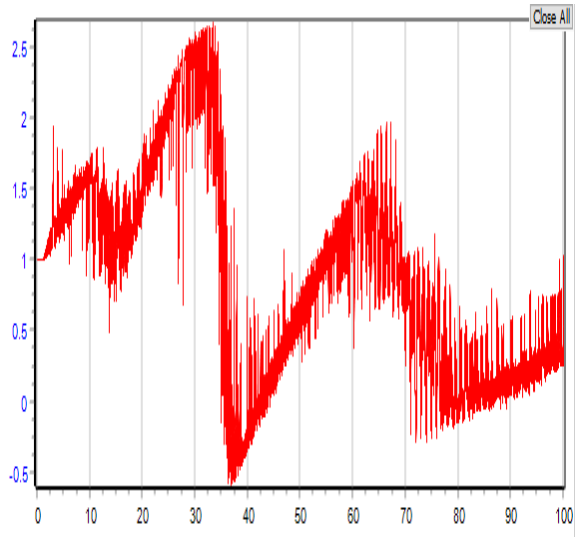

Figure 12: Afam IV 132kV bus and rotor angle was faulted with 3-phase to ground fault for 150 ms.

4.7 Effect of Substation Splitting on Transient Stability

After splitting Afam V and Afam III generators, a transient three -Phase fault was added, simulated on the Afam V 132kV bus to look at the impact of splitting on bus frequency and angle. Figure 12 shows the transient stability plot of the bus frequencies on the remaining plants, while the angles of the bus are shown in Figure 13. This demonstrates the structure's stability, when splitting is used, it improves.

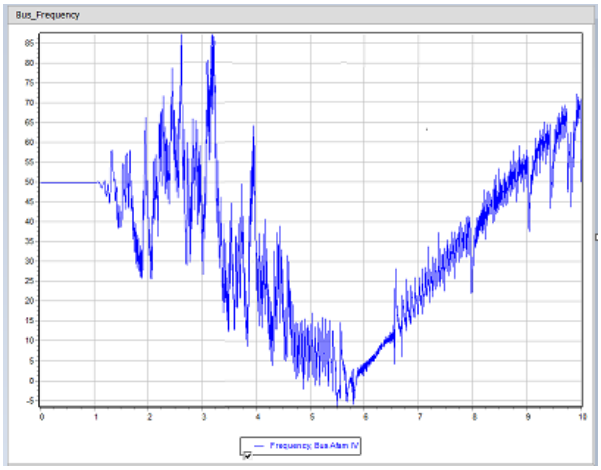

Figure 13: Afam III, IV and V bus frequency and clearing time 100ms

4.8 Contingency Analysis

Only the N-1 criterion was considered to evaluate the contingencies in this work. With one circuit, one generating plant removed, the power flow experiments were replicated. It looked into the impact's effect of the removal on the system. The effect of this elimination of the producing plant was seen in the sharing between the other generating plants of the load it normally supplies, thereby raising their loads. The loading on almost all of the contingency events considered was certain neighboring lines have changed slightly. A significant concern of this removed generator was that the retained Afam IV-Afam V line had an increase from 85.6 percent to 98.8 percent loading.

Table 8: Result of the Contingency Analysis

Number	Gen zone	category	Value	Limit	Percent	Limit	Nom kV
1	Afam (IV)	Bus low Volts	0.7371	0.900	81.90	No	0.900
2	Afam (V-)	Bus low Volts	0.7525	0.900	83.61	No	0.900
3	Onne (7)	Bus low Volts	0.7529	0.900	83.66	No	0.900
4	Rivers IPP (4)	Bus low Volts	0.7529	0.900	80.16	No	0.900
5	Afam (IV)	Bus low Volts	0.6353	0.900	70.72	No	0.900
6	Alaoji (6)	Bus low Volts	0.6545	0.900	72.78	No	0.900
7	Onne (7)	Bus low Volts	0.655	0.900	72.72	No	0.900
8	Rivers IPP (4)	Bus low Volts	0.6191	0.900	68.79	No	0.900
9	Afam (IV)	Bus low Volts	0.5297	0.900	58.86	No	0.900
10	Alaoji (6)	Bus low Volts	0.5489	0.900	60.05	No	0.900
11	Onne (7)	Bus low Volts	0.5489	0.900	61.05	No	0.900
12	Rivers IPP (4)	Bus low Volts	0.5139	0.900	57.10	No	0.900

Table 9: the violations when Afam III is opened

Number	category	Element	Value	Limit	Percent	Area Name	Nom kV
1	Bus low Volts	Rivers IPP (4)	0.8993	0.900	99.93	1	132
2	Bus low Volts	Afam (IV)	0.6923	0.900	76.92	1	132
3	Bus low Volts	Alaoji (6)	0.5812	0.900	64.58	1	132
4	Bus low Volts	Onne (7)	0.4784	0.900	53.16	1	132

6. CONCLUSION

The successful studies for evacuation of power from existing generators in Rivers State Nigeria was carried out in this analysis; details of the technical information of the plants were gotten from TCN (Transmission Company of Nigeria). Power flow studies, loading of equipment, short circuit studies, transient stability studies, and N-1 criterion studies were conducted to study the system. The power flow studies described the system's voltage profile. Equipment loading demonstrates the capacity-carrying devices. According to the short circuit studies, several power station buses are flowing from the fault. Stability of the system is maintained after 7.5 cycles of exposure to a transient fault, according to transient stability experiments. The transmission, as observed from the contingency study, capacity in Afam IV cannot withstand N-1 criterion if the three generators fail; thus, there is a requirement to increase the generators' generation capacity to avoid overloading and ultimate generator failure.

7. REFERENCES

[1] Emovon, I., Samuel, O. D., Mgbemena, C. O., and Adeyeri, M. K. (2018). Electric Power generation crisis in Nigeria: A Review of causes and solutions. International Journal of Integrated Engineering, 10(1), 1–20. https://doi.org/10.30880/ijie.2018.10.01.008

[2] Ohajianya, A. C., Abumere, O. E., Owate, I. O., and Osarolube, E. (2014). Erratic Power Supply in Nigeria: Causes and Solutions. International Journal of Engineering Science Invention, 3(71), 51–55.

[3] Opec

[4] Oyedepo, S. O., Babalola, O. P., Nwanya, S. C., Kilanko, O., Leramo, R. O., Aworinde, A. K., … Agberegha, O. L. (2018). Towards a Sustainable Electricity Supply in Nigeria: The Role of Decentralized Renewable Energy System. European Journal of Sustainable Development Research, 2(4), 6–8. https://doi.org/10.20897/ejosdr/3908

[5] Oleka, E. U., Ndubisi, S. N., and Ijemaru, G. K. (2016). Electric Power Transmission Enhancement: A Case of Nigerian Electric Power Grid. American Journal of Electrical and Electronic Engineering, 4(1), 33–39. https://doi.org/10.12691/ajeee-4-1-5

[6] World Bank. (2014). Market Information Nigeria Energy Sector. Retrieved 2014, from https://data.worldbank.org/indicator/EG.USE.ELEC.KH.PC

[7] Ralte, R. (2003). Design Of 132 kV Power Evacuation System at Bawktlang Substation in Mizoram. http://hdl.handle.net/123456789/11947

[8] Abdullahi, H., Muhammad, B., and Muhammad, S. (2015). An Optimal Analysis of Power Evacuation in Tiga Hydro Power Plant in Kano State.

[9] Soni, S., S.K. Bajpai, S. K., and Chauhan, R. (2013). Optimum Power Evacuation System Planning of Malwa Thermal Power Station (Stage –II, 2x660MW). International Journal of Advancements in Research & Technology, 2(12).

[10] Adetona, S., Ugwuagbo, E., Okafor, F., and Akinbulire, T. (2018). Modelling of an Electric Power Grid for New Power Plant Evacuation. FUOYE Journal of Engineering and Technology, 3(2). https://doi.org/10.46792/fuoyejet.v3i2.219

[11] Somolu, F.A. and Okafor, F.N. (2007). Integration and Evacuation Studies for National Integrated Power Projects (NIPP). NIPP Inhouse grid study steam/PHCN.

[12] Abdullahi, H., Muhammad, B. and Muhammad, S. (2015b, September). An Optimal Analysis of Power Evacuation in Tiga Hydro Power Plant in Kano State. 2nd International Conference on Science, New Delhi, India.

[13] Gaya, S, et al. Recent Review on Load/Power Flow Analysis. international Journal of Scientific and Engineering Research, Dec. 2020.

[14] Kumar, Nitesh and Samina Mubeen. “A Review on Load Flow Analysis.” Ijird, Nov. 2014.

[15] SURESH, V. (2019). Load Flow Analysis in local microgrid with storage. Przegląd Elektrotechniczny, 1(9), 100–104. https://doi.org/10.15199/48.2019.09.19

[16] Saadat, M. (1978). Application of quasi-Newton method to load flow studies and solution of load flow during three-phase fault. Electric Power Systems Research, 1(3), 173–179. https://doi.org/10.1016/0378-7796(78)90021-4

[17] Wu, X., and Mutale, J. (2003). An investigation of network splitting for fault level reduction. Tyndall Centre for Climate Change Research. Published.

[18] Sharma, A., Nirwan, A., and Shekhawat, A. S. (2017). Fault Analysis on Three Phase Transmission Lines and its Detection. International Journal of Advance Research and Innovation, 5(2).

[19] Abduulkareem, A., Awosope, C. O. A., and Awelewa, A. A. (2016). The Use of Three-Phase Fault Analysis for Rating Circuit Breakers on Nigeria 330kv Transmission lines. Journal of Engineering and Applied Sciences, 11(12), 2612–2621.

[20] Anwar, N., Hanif, A. H., Khan, H. F., and Ullah, M. F. (2020). Transient Stability Analysis of the IEEE-9 Bus System under Multiple Contingencies. Engineering, Technology & Applied Science Research, 10(4), 5925–5932. https://doi.org/10.48084/etasr.3273

[21] Wang, H., and Li, Z. (2019). A Review of Power System Transient Stability Analysis and Assessment. 2019 Prognostics and System Health Management Conference (PHM-Qingdao). Published. https://doi.org/10.1109/phm-qingdao46334.2019.8942834

[22] Bulat, H., Franković, D., and Vlahinić, S. (2021). Enhanced Contingency Analysis—A Power System Operator Tool. Energies, 14(4), 923. https://doi.org/10.3390/en14040923

[23] Alam, M. (2020). Evaluation Of N-1 Contingency Ranking for Security Analysis in Modern Power System. Ethics and Information Technology. Published. https://doi.org/10.26480/etit.02.2020.154.157

[24] Igbinovia, F. O. (2014). A Review of Electrical Energy Systems in Nigeria: Proposal to Increase Consumption. A Review of Electrical Energy Systems in Nigeria: Proposal to Increase Consumption, 1–4. Retrieved from https://www.academia.edu/34444954/A_Review_Of_Electrical_Energy_Systems_In_Nigeria_Proposal_To_Increase_Consumption